



Contents lists available at SCCE

Journal of Soft Computing in Civil Engineering

Journal homepage: www.jsftcivil.com



A Comparative Study of Shearlet, Wavelet, Laplacian Pyramid, Curvelet, and Contourlet Transform to Defect Detection

Sepideh Vafaie^{1*} , Eysa Salajegheh²

1. Ph.D. Student, Faculty of Earth and Environmental Studies, Montclair State University, United States

2. Professor, Faculty of civil Engineering, Shahid Bahonar University of Kerman, Kerman, Iran

Corresponding author: vafaies1@montclair.edu

 <https://doi.org/10.22115/SCCE.2023.356475.1505>

ARTICLE INFO

Article history:

Received: 16 August 2022

Revised: 04 January 2023

Accepted: 31 January 2023

Keywords:

Wavelet transform;

Laplacian pyramid transform;

Curvelet transform;

Contourlet transform;

Shearlet transform;

Damage detection.

ABSTRACT

This study presents a new approach based on shearlet transform for the first time to detect damages, and compare it with the wavelet, Laplacian pyramid, curvelet, and contourlet transforms to specify different types of defects in plate structures. Wavelet and Laplacian pyramid transforms have inferior performance to detect flaws with different multi-directions, such as curves, because of their basic element form, expressing the need for more efficient transforms. Therefore, some transforms, including curvelet and contourlet, have been evaluated so far for improving the performance of traditional transforms. Although these transforms have overcome the deficiencies of previous methods, they have a weakness in detecting several imperfections with various shapes in plate structures—one of the essential requirements that each transform should possess. In this study, we have used the shearlet transform that is used for the first time to detect identification and overcome all previous transform dysfunctions. In this regard, these transforms were applied to a four-fixed supported square plate with various defects. The obtained results revealed that the shearlet transform has the premier capability to demonstrate all kinds of damages compared to the other transforms, namely wavelet, Laplacian pyramid, curvelet, and contourlet. Also, the shearlet transform can be considered as an excellent and operational approach to demonstrate different forms of defects. Furthermore, the performance and correctness of the transforms have been verified via the experiment.

How to cite this article: Vafaie S, Salajegheh E. A comparative study of shearlet, wavelet, laplacian pyramid, curvelet, and contourlet transform to defect detection. *J Soft Comput Civ Eng* 2023;7(2): 1–42. <https://doi.org/10.22115/scce.2023.356475.1505>

2588-2872/ © 2023 The Authors. Published by Pouyan Press.

This is an open access article under the CC BY license (<http://creativecommons.org/licenses/by/4.0/>).



1. Introduction

Non-destructive methods in civil engineering (e.g., wavelet transform) have received significant attention in recent decades [1]. In the past few years, the application of wavelet transforms for health monitoring of structures (SHM) and detecting damages have been investigated by many researchers. Ovanosova and Suarez [1] used wavelet transform to find defects in frame structures, showing that this method merely needs response data of the defective structure. Kim and Melhem [2] offered the wavelet analysis method for defect identification. They first presented the theory of wavelet transform and then used it in the detection of cracks in a beam and mechanical gear. Yun et al. [3] proposed a technique based on analyzing the wavelet signal of the smart wireless sensor for the identification of the decentralized defect. They verified this proposed method with experimental tests. Bagheri et al. [4] expressed the ability of a two-dimensional discrete wavelet transform to identify damage of plates using modal data. Also, they used experimental data to validate the proposed technique. Cao et al. [5] suggested the utilization of the Teager energy operator along with wavelet transform for beam damage recognition in noisy conditions. They applied this method on several analytical cases to show the competence of their proposed technique. Yang and Nagarajaiah [6] suggested the blind damage detection by analyzing independent component via wavelet transform. Moreover, examples of the seismic-excited structures are stated to indicate the ability of the developed method. Ulriksen et al. [7] developed a new technique based on wavelet transform and modal analysis to identify defects of wind turbine blades. Shahsavari et al. [8] presented the mode shape analysis with wavelet transform to detect defects of beams. Wang et al. [9] introduced a new form of wavelet transform based on residual force vector for fault recognition of underground tunnel structures. They introduced a novel damage index, which can be used as an efficient defect detection indicator. Zhu et al. [10] proposed an approach for crack recognition using continuous wavelet transform through introducing a new index for defect discernment. Jahangir et al. [11] presented an approach based on wavelet analysis to identify damage to RC beams. Fakharian and Naderpour [12] utilized two various methods including wavelet packet transform and peak picking to assess the quantification of defect severity. Naderpour et al. [13] presented shear strength prediction using three different approaches including ANN, GMDH-NN, and GEP. They showed all of the methods are capable of predicting properly. Ghanizadeh et al. [14] used evolutionary polynomial regression to develop a prediction model for collapse settlement and stress release coefficients. Naderpour et al. [15] utilized a new approach based on the data handling group method to the estimation of the moment capacity of ferrocement members. Bagheri and Kourehli [16] presented a wavelet analysis based-method to defect identification. Kourehli [17] used wavelet transform to structural health monitoring of steel frames. Ghannadi and Kourehli [18] used a slim mold algorithm to damage detection. Ghannadi and Kourehli [19] suggested a new method based on a moth-flame algorithm to defect identification. Also, there are some useful methods including wavelet transform and optimization that have been used recently for damage demonstration [20–23]. Another transform that has been evaluated in this investigation is the Laplacian pyramid transform. Burt and Adelson [24] suggested the new method based on the

Laplacian pyramid, well suited for image analysis and compression. Also, Do and Vetterli [25] used the Laplacian pyramid to create a new transform, named pyramid directional filter bank. They demonstrated that once the Laplacian pyramid is applied on a signal, two parts are produced, including approximation and detail. Although wavelets have been widely utilized in damage detection, they have offered a poor performance on representing objects with highly anisotropic elements. Accordingly, other transforms have been introduced to overcome the weakness of traditional approaches. In what follows, some of these transforms are expressed. Candes et al. [26] presented the fast discrete curvelet transform, i.e., the second generation of curvelet transform. Bagheri et al. [27] used the curvelet transform for recognition of vibration-based defects of plate structures, demonstrating its excellent ability to show line features. Nicknam et al. [28] propounded curvelet transform via wrapping procedure for fault discernment in two-dimensional structures. They used both numerical and experimental data to display the superior performance of this technique. Another transform that has been developed to improve the traditional multiscale representation is the contourlet transform. Do and Vetterli [29] proposed a new two-dimensional image representation named the contourlet transform. Po and Do [30] exhibited that contourlets are composed of basics oriented at various directions, which enables this transform to show smooth contours of natural images effectively. Vafaie and Salajegheh [31] compared wavelet and contourlet transforms for the identification of vibration-based damage of plate structures, showing the superiority of contourlets over wavelets in the detection of curved cracks in the plate structures. Jahangir et al. [32] proposed using contourlet transform to damage localization and assessment of severity. Although these transforms have been successful in overcoming the weakness of the previous techniques, they could not detect damages with various shapes excellently. Thus, the shearlet transform has been presented as an efficient technique in this study. Lim [33] suggested the discrete shearlet transform, utilized to provide efficient multiscale directional representation. Xu et al. [34] applied the shearlet transform for the surface defects classification of metals. They expressed that since various damages have information in several directions and on different scales, another transform superior to wavelet should be used, i.e., the shearlet transform.

2. Research significance

This investigation mainly aims to present the effectiveness of a shearlet transform-based approach which is used for the first time to defect detection, and compared to the wavelet, Laplacian pyramid, curvelet, and contourlet transforms, to detect imperfections with various shapes in plate structures. Thus, eight examples with multiple damages have been discussed to check the transform performance. The rest of this paper is organized as follows. In section 2, the overview of the algorithm of wavelet, Laplacian pyramid, curvelet, contourlet, and shearlet transforms is presented. Then, the process of defect identification with these five transforms is expressed, and a damage index is also introduced to show flaws. In section 3, eight numerical examples are addressed. Performance evaluation of the transforms through an experimental model is carried out in section 4. Finally, section 5 represents the concluding remarks.

3. Methods

Defect detection with wavelet, Laplacian pyramid, curvelet, contourlet, and shearlet transforms includes the following steps:

- Model a plate
- Obtain the structural response of the plates
- De-noise the structural response of the plates
- Apply the transforms
- Determine the damage index (DI)
- Plot the damage index

These steps are presented comprehensively as below:

3.1. Model a plate

In this part, the plate with and without damage is simulated. A defect in the plate can be modeled as the reduction of cross-sectional area, material properties, stiffness, and so forth. In this research, the flaw is simulated as the reduction of Young's modulus in the damaged plate. As can be seen in Eq. (1), Young's modulus for damaged plate is denoted by $E_{damaged}$, where d stands for the intensity of defect, and $E_{undamaged}$ is Young's modulus of the undamaged plate. It is worth mentioning that d could be located between 0 and 1 (in our examples 0.05, 0.1, and 0.2 was considered). In addition, d is equal to 0 and 1 meaning undamaged and fully damaged states, respectively.

$$E_{damaged} = E_{undamaged}(1 - d) \quad (1)$$

3.2. Obtain the structural response of the plates

After modeling a plate, the structural response of the plate is required for fault identification. In this investigation, the plate mode shape was used to obtain the displacement of nodes in the fundamental mode shape of the plate as the structural response needed for the procedure of damage identification. It is worth noting that the finite element method (FEM) was implemented to specify the plate mode shape. The equation of free vibration is defined as:

$$M\ddot{u}(t) + Ku(t) = f(t) \quad (2)$$

Where M , K , and f are the mass, stiffness matrices, and force vector, respectively. Also, \ddot{u} and u are acceleration and displacement, respectively. According to the harmonic motion, the natural frequencies and the modes of vibration are gained as

$$K - \omega_i^2 M) \varphi_i = 0, \quad i = 1, 2, \dots, n_m \quad (3)$$

Where ω_i is the natural frequency, φ_i is the i th vibration mode shape vector, and n_m is the structural modes number [35].

3.3. De-noise the structural response of the plates

Since measured data of the structures contain noise in a real experiment, de-noising plays an essential role in the process of defect recognition. However, the noise amount is ambiguous, and, in turn, it is likely to delete useful information containing noise in the process of de-noising the measured information with low noise. Therefore, de-noising is one of the significant sections in the defect detection process. In this study, de-noising was performed as follows:

1. The transform was applied to the signal (the displacement in the plate fundamental mode shape) to obtain the transform coefficients.
2. Set the coefficient threshold.
3. De-noised coefficients were utilized to reconstruct the de-noised signal.

It should be noted that the white Gaussian noise has been added to the signal randomly.

$$Z_i \sim \mathcal{N}(0, N) \quad (4)$$

$$Y_i = X_i + Z_i$$

Where Z_i is drawn from a normal distribution with a mean value of zero and the variance N , and it adds the noise randomly to our signal which is X_i . In addition, we have compared two various methods based on wavelet sym4 and db1 to denoise the noisy signal, and we have used sym4 according to the superior performance of sym4 [36].

3.4. Apply the transforms

In this section:

- a) An overview of the wavelet, Laplacian pyramid, curvelet, contourlet, and shearlet transform is given.
- b) Then, the structural response of the plates —considered as the displacement of the nodes in the first mode shape of the plates in this study— is utilized as a signal for these transforms to acquire the transform detail coefficients.
- c) Finally, these detail coefficients are used in the next stage in the damage index for defect detection.

In all formulas, the following notations are used:

- ✓ j = decomposition level of the transform
- ✓ l = number of directions for displaying detail coefficients, $l = 0, 1, \dots, L$
- ✓ low-pass of signal = approximation part; high-pass of signal = detail part

3.4.1. Wavelet transform

Two parts are produced by applying two-dimensional wavelet to a signal for $j = J$; approximation (cA_j) and three detail coefficients $(cD_j^{horizontal, l=1}, cD_j^{vertical, l=2}, cD_j^{diagonal, l=3}, l = 1, 2, 3 (L = 3))$ (Fig. 1).

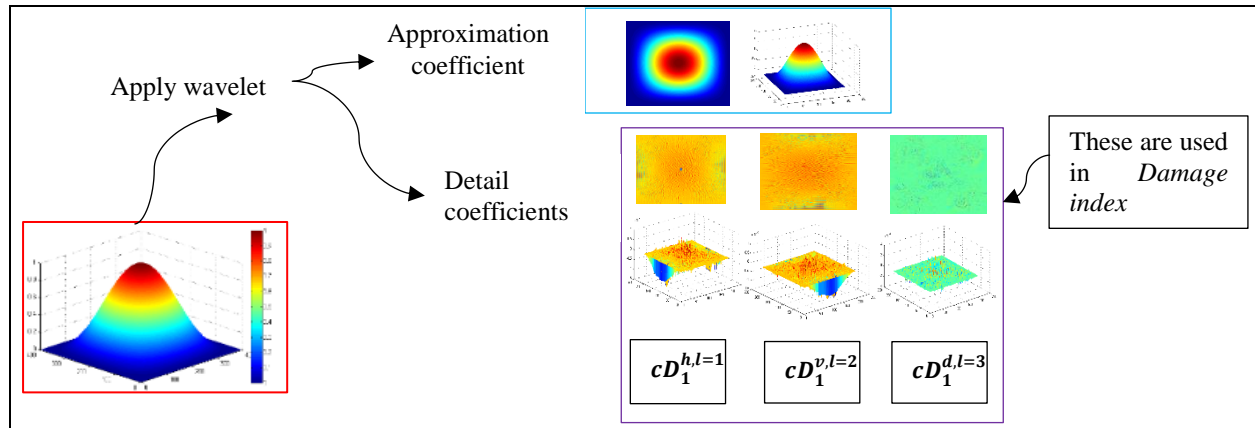


Fig. 1. The scheme of wavelet transform for damage detection with an example for $j=1$.

Also, as choosing the proper wavelet is very important due to its significant impact on damage identification, in this study, three wavelets – Haar, Symlet, and Discrete Meyer – are used to compare their performance and choose the one having the superior efficiency in detecting a flaw.

Haar wavelet: The Haar wavelet is a rescaled function sequence (square-shaped) that form a wavelet family. The Haar wavelet mother and its scaling function— $\psi(x)$, $\phi(x)$ —are determined as follows [35]:

$$\psi(x) = \begin{cases} 1 & 0 \leq x < 0.5 \\ -1 & 0.5 \leq x < 1 \\ 0 & \text{otherwise} \end{cases} \quad (5)$$

$$\phi(x) = \begin{cases} 1 & 0 \leq x \leq 1 \\ 0 & \text{otherwise} \end{cases} \quad (6)$$

Symlet wavelet: The family of Symlet wavelets is a modified version of Daubechies wavelets with increased symmetry [37]. The mother wavelet and scaling function are represented in Fig. 2.

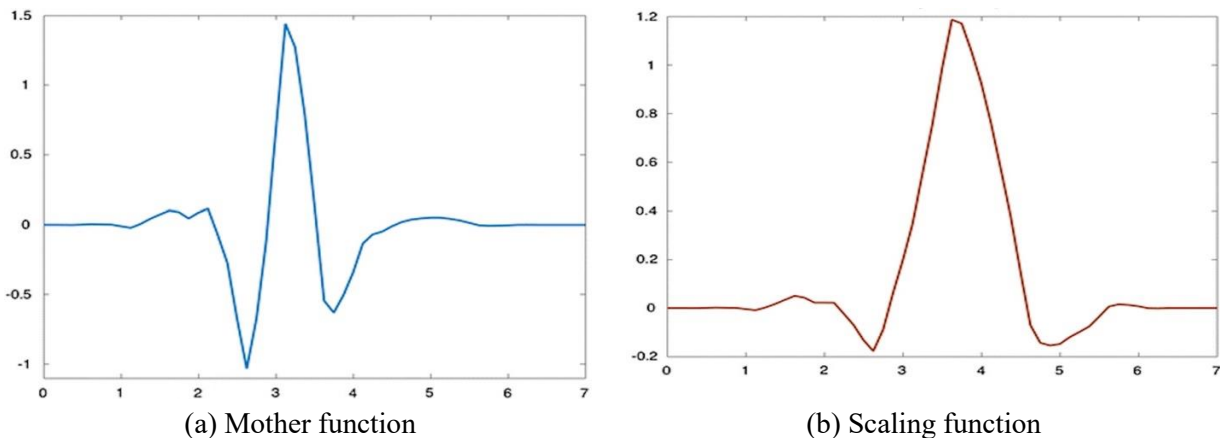


Fig. 2. Symlet wavelet function [38].

Discrete Meyer wavelet: The Meyer wavelet is infinitely differentiable with infinite support; defined in the frequency domain in terms of function ν as [39]:

$$\psi(\omega) := \begin{cases} \frac{1}{\sqrt{2\pi}} \sin\left(\frac{\pi}{2} v\left(\frac{3|\omega|}{2\pi} - 1\right)\right) e^{j\omega/2} & \text{if } \frac{2\pi}{3} < |\omega| < \frac{4\pi}{3} \\ \frac{1}{\sqrt{2\pi}} \cos\left(\frac{\pi}{2} v\left(\frac{3|\omega|}{4\pi} - 1\right)\right) e^{j\omega/2} & \text{if } \frac{4\pi}{3} < |\omega| < \frac{8\pi}{3} \\ 0 & \text{otherwise} \end{cases} \quad (7)$$

$$v(x) := \begin{cases} 0 & \text{if } x < 0 \\ x & \text{if } 0 < x < 1 \\ 1 & \text{if } x > 1 \end{cases} \quad (8)$$

In this investigation, all three above wavelets are evaluated in the second numerical example.

3.4.2. Laplacian pyramid and Contourlet transform

Contourlet transform is a multiresolution transform with basic functions $\psi_{a,j,l}^n$. Thus, the contourlet transform of a signal is determined as:

$$Ccont(a, j, l, n) = \langle signal, \psi_{a,j,l}^n \rangle \quad (9)$$

Where $Ccont(a, j, l, n)$ is the inner product of signal with the basic functions ($\psi_{a,j,l}^n$); $a, a > 0$ scale; $n =$ decomposition levels number of the directional filter bank. Also, $Ccont(a, j, l, n)$ determines coefficients of the contourlet transform, which includes high and low-frequency parts, see [25] for more information. In this study, we considered an effective discrete contourlet transform scheme based on a Laplacian pyramid combined with proper directional filter banks, which was proposed in [29], (section a=Laplacian pyramid transform, section(a+b)= contourlet transform).

Section a) First, Laplacian pyramid transform is applied to a signal. After the Laplacian pyramid stage, the output is J high-pass signal $cD_j^{l=1}$, $j = 1, 2, \dots, J$; $L = 1$) (in the fine to coarse order) and a low-pass signal cA_j .

Therefore, by applying Laplacian pyramid on a signal for $j = J$, two parts are produced; approximation (cA_j) and detail coefficient ($cD_j^{l=1}$, $L = 1$). In this study, as indicated in Fig. 3, Laplacian pyramid transform is applied on the structural response of the intact and imperfect plate, which is the node displacement in the plate initial mode shape, to generate the detail coefficient. In the next step, the detail coefficient ($cD_j^{l=1}$, $L = 1$) is used as $cD_{damaged}^l$ (detail coefficients of the damaged plate) and $cD_{undamaged}^l$ (detail coefficients of the undamaged plate) in section 3.5. Damage index, Eq. 15. Fig. 3 illustrates the Laplacian pyramid transform decomposition for $j=1$.

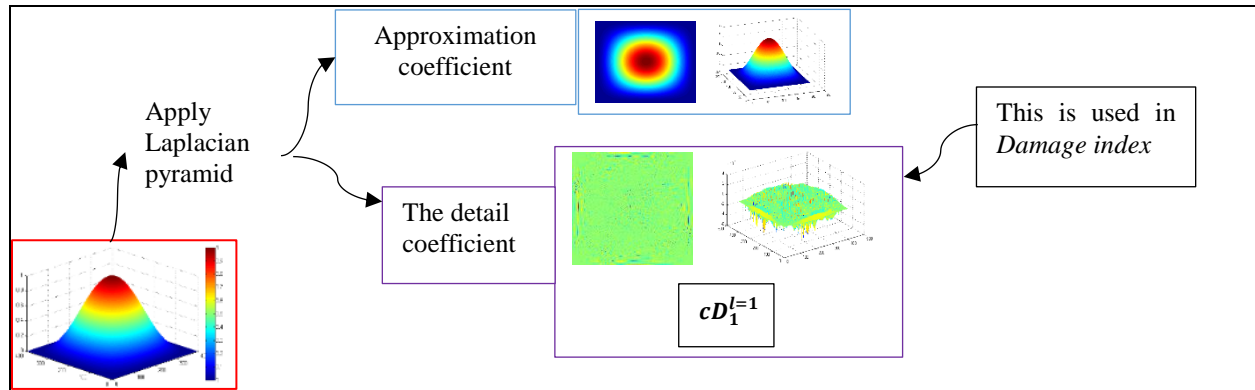


Fig. 3. The scheme of Laplacian pyramid transform for damage detection with an example for $j=1$.

Section b) Second, a directional filter bank is applied on $cD_j^{l=1}$, $L = 1$ (high-pass signal). Each high-pass signal $cD_j^{l=1}$, $j = 1, 2, \dots, J$; $L = 1$ is further decomposed by a directional filter bank into l high-pass directional signal (cD_j^l , $l = 1, 2, \dots, L$), (cA_j approximation coefficient, and cD_j^l , detail coefficients) [29].

Therefore, by applying contourlet transform to a signal for $j = J$, two parts are produced; approximation (cA_j) and detail coefficient (cD_j^l), $l = 1, 2, \dots, L$ (contourlet can show details in various directions). In this research, as demonstrated in Fig. 4, the contourlet transform is applied to the structural response of flawless and imperfect plate, the node displacement in the fundamental mode shape, to produce the detail coefficients. In the next step, the detail coefficients (cD_j^l , $l = 1, 2, \dots, L$) are utilized as $cD^l_{damaged}$ (detail coefficients of the damaged plate) and $cD^l_{undamaged}$ (detail coefficients of the undamaged plate) in section 3.5. Damage index, Eq. 15. Fig. 4 indicates the decomposition of contourlet transform when $j=1$, $L=4$.

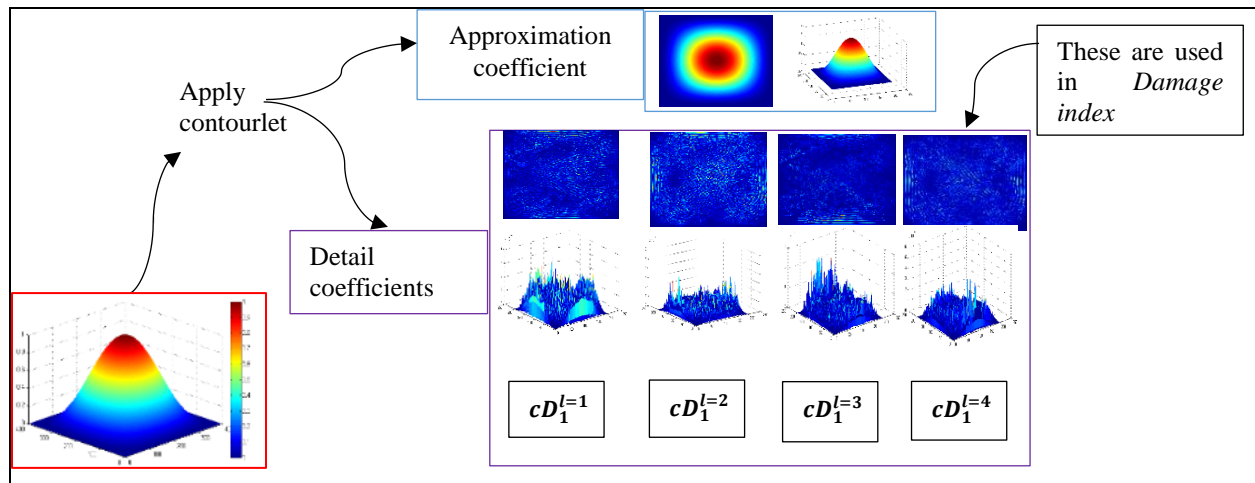


Fig. 4. The scheme of contourlet transform for damage detection with an example for $j=1$, $L=4$.

Also, selecting the appropriate Laplacian filter is very important in contourlet and Laplacian pyramid transforms for damage identification. Accordingly, 9/7 wavelet filter bank and PKVA filter (filters from the ladder structure) are utilized in this study in the second example.

3.4.3. Curvelet transform

Curvelets consists of the two forms of block ridgelet transform and curvelet transform on the Fourier domain. In block ridgelet transform, signals are segmented into blocks, and ridgelet is performed on the blocks. In the curvelet transform, frequency partitioning is performed on the frequency domain. Therefore, the curvelet transform of a signal with basic functions $\psi_{a,j,l}^p$ is defined as:

$$Ccurv(a, j, l, p) = \langle signal, \psi_{a,j,l}^p \rangle \tag{10}$$

Where $Ccurv(a, j, l, p)$ is the inner product of *signal* with the basic functions ($\psi_{a,j,l}^p$); $a, a > 0$ scale; $p = (p_1, p_2) \in Z^2$ the sequence of translation parameters. Also, $Ccurv(a, j, l, p)$ determines the coefficients of the curvelet transform, including high and low-frequency parts, see ([40]; [26]) for more information. In this research, digital curvelet transform is considered as the following:

$$Signal = cA_j + \sum_{j=1}^L cD_j^l, \quad l = 1, 2, \dots, L \tag{11}$$

Where cA_j is a low pass version of the signal (approximation part), and $cD_j^l, l = 1, 2, \dots, L$ represents details of the signal, see [26] for more information. Therefore, by applying curvelet transform on a signal for $j = J$, two parts of approximation (cA_j) and detail coefficient (cD_j^l), $l = 1, 2, \dots, L$ (curvelet can exhibit details in several directions) are produced. In this investigation, as exhibited in Fig. 5, the curvelet transform is applied to the structural response of intact and imperfect plate to generate the detail coefficients. In the next step, the detail coefficients ($cD_j^l, l = 1, 2, \dots, L$) are used as $cD_{damaged}^l$ (detail coefficients of the damaged plate) and $cD_{undamaged}^l$ (detail coefficients of the undamaged plate) in section 3.5. Damage index, Eq. 15. Fig. 5 demonstrates the curvelet transform decomposition when $j=1, L=4$.

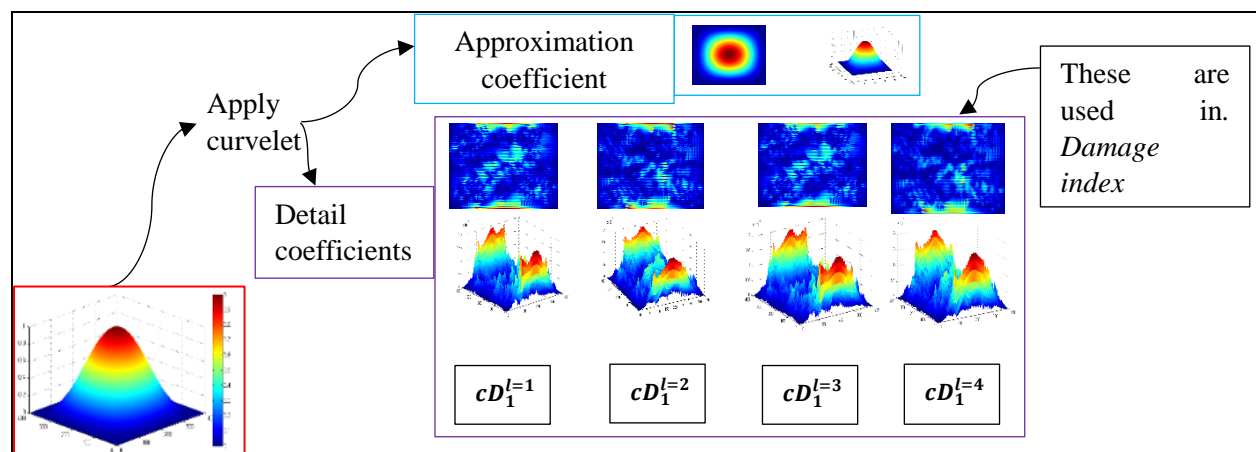


Fig. 5. The scheme of curvelet transform for damage detection with an example for $j=1, L=4$.

3.4.4. Shearlet transform

The shearlet transform is a multiresolution transform with basic functions $\psi_{a,b,s}$ defined as:

$$\psi_{a,b,s}(x) = a^{-\frac{3}{4}} \psi(A_a^{-1} S_s^{-1}(x - b)) \tag{12}$$

$$A_a = \begin{pmatrix} a & 0 \\ 0 & \sqrt{a} \end{pmatrix}, \quad S_s = \begin{pmatrix} 1 & s \\ 0 & 1 \end{pmatrix} \quad (13)$$

Where a , $a > 0$ is scale; $b \in \mathbb{R}^2$ is position; $s \in \mathbb{R}$ is the slope in the frequency domain; A_a is parabolic scaling matrix; and S_s is the shear matrix. Therefore, the shearlet transform of a signal is defined as:

$$Cshear(a, b, s) = \langle signal, \psi_{a,b,s} \rangle \quad (14)$$

Where $Cshear(a, b, s)$ is the inner product of signal and the basic functions ($\psi_{a,b,s}$). Also, $Cshear(a, b, s)$ defines the coefficients of the shearlet transform, which includes high and low-frequency parts ([41]; [42]). In this study, a discrete shearlet transform was considered, which included the Laplacian pyramid and shearing filters [34]. First, the Laplacian pyramid transform was applied to a signal where the outputs consisted of J high-pass signal $cD_j^{l=1}$, $j = 1, 2, \dots, J$; $L = 1$ and low-pass signal cA_j . Second, proper shearing filters were applied to $cD_j^{l=1}$, $L = 1$, (high-pass signal) to generate l high-pass directional signal (cD_j^l , $l = 1, 2, \dots, L$); (cA_j defines approximation coefficient, and cD_j^l defines detail coefficients in l directions). Therefore, by applying shearlet transform to a signal for $j = J$, two parts are produced; approximation (cA_j) and detail coefficient (cD_j^l), $l = 1, 2, \dots, L$ (shearlets are capable of demonstrating details in various directions). In this study, as demonstrated in Fig. 6, the shearlet transform is applied to the structural response of damaged and undamaged plates, i.e., the node displacement in the initial mode shape of the plates, to produce the detail coefficients. In the next step, the detail coefficients (cD_j^l , $l = 1, 2, \dots, L$) were used as $cD_{damaged}^l$ (detail coefficients of the damaged plate) and $cD_{undamaged}^l$ (detail coefficients of the undamaged plate) in section 3.5. Damage index, Eq. 15. Fig. 6 displays shearlet transform decomposition when $j=1$, $L=6$.

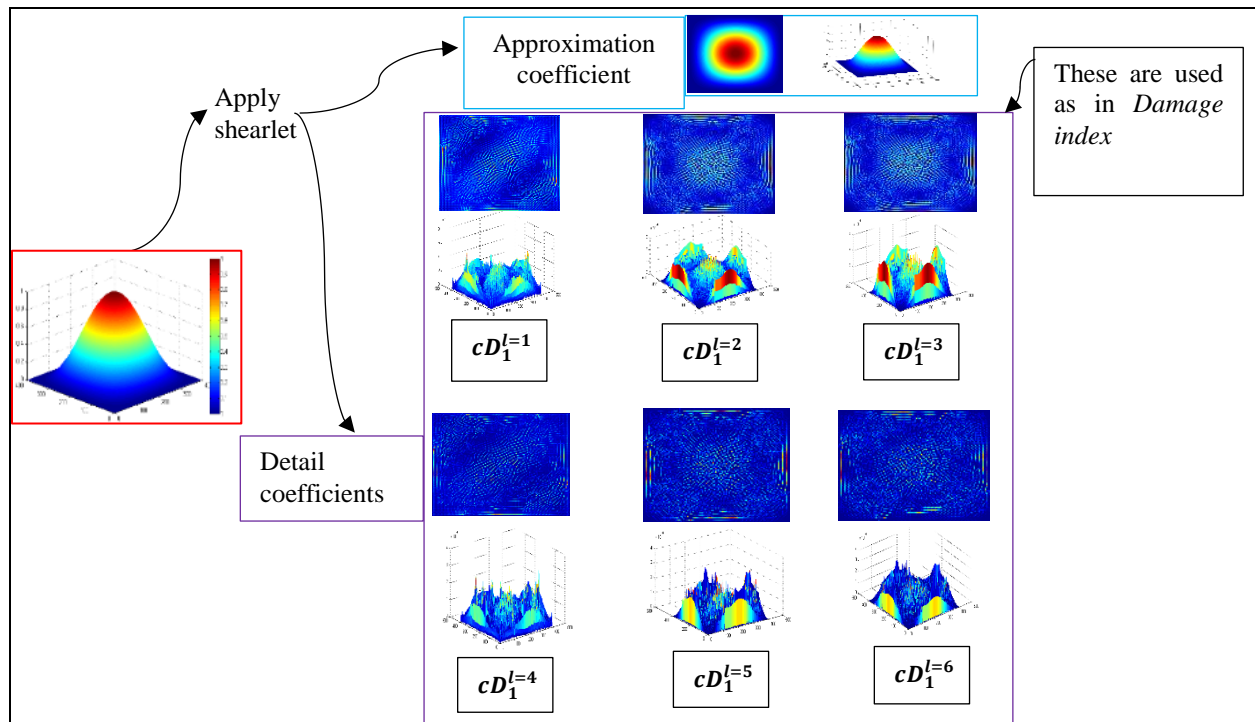


Fig. 6. The scheme of shearlet transform for damage detection with an example for $j=1$, $L=6$.

3.5. Determine the damage index (DI)

The specification of the appropriate connection, named as damage index, is a central part of the flaw identification process [14]. Accordingly, after obtaining detail coefficients of the damage and undamaged plates, a proper relationship was defined between both of them that led to the efficient demonstration of the defect place. The damage index is defined as follows:

$$DI = \sqrt{\frac{\frac{1}{L} \sum_{l=1}^L (cD_{damaged}^l - cD_{undamaged}^l)^2}{\frac{1}{L} \sum_{l=1}^L (cD_{undamaged}^l)^2}} \quad (15)$$

$cD_{damaged}^l$, and $cD_{undamaged}^l$ determine the detail coefficients of the transforms for the damaged and undamaged plates, respectively.

3.6. Plot the damage index

Finally, the defect location was obtained for each transform by plotting the damage index. In other words, the defect location was determined as the maximum value of the damage index in all transforms. As indicated in Fig. 7, the fault detection procedure was identical for all transforms.

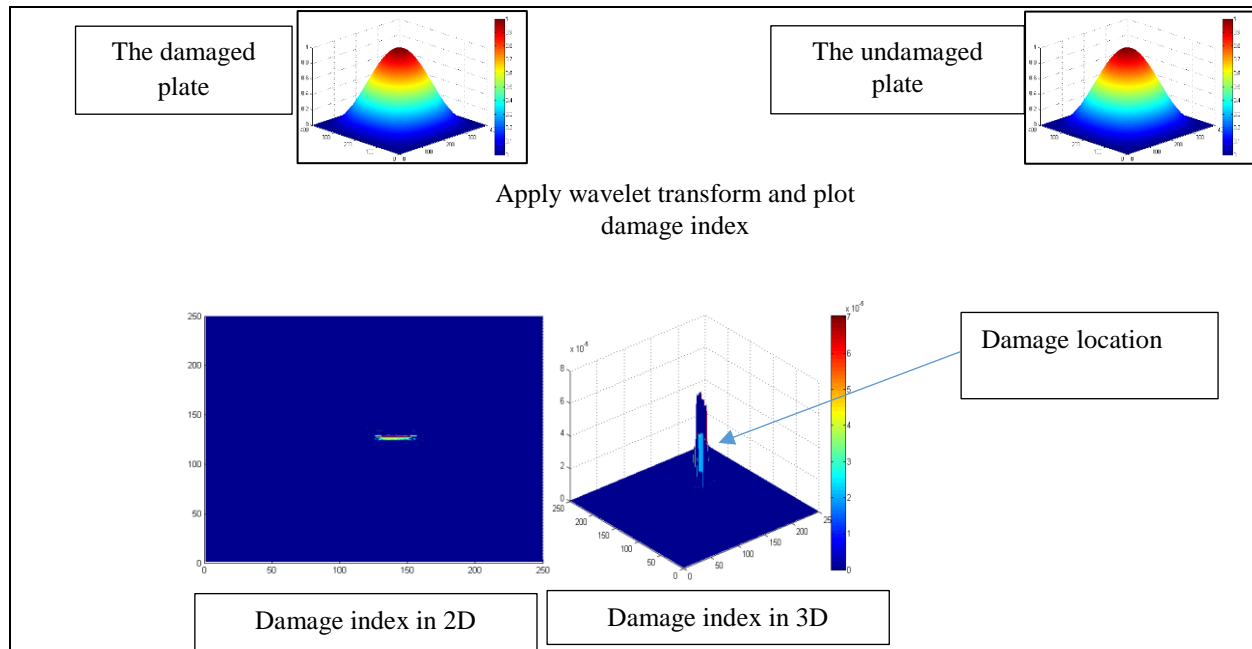


Fig. 7. The general procedure of damage detection using the structural response for the horizontal linear defect example.

4. Results

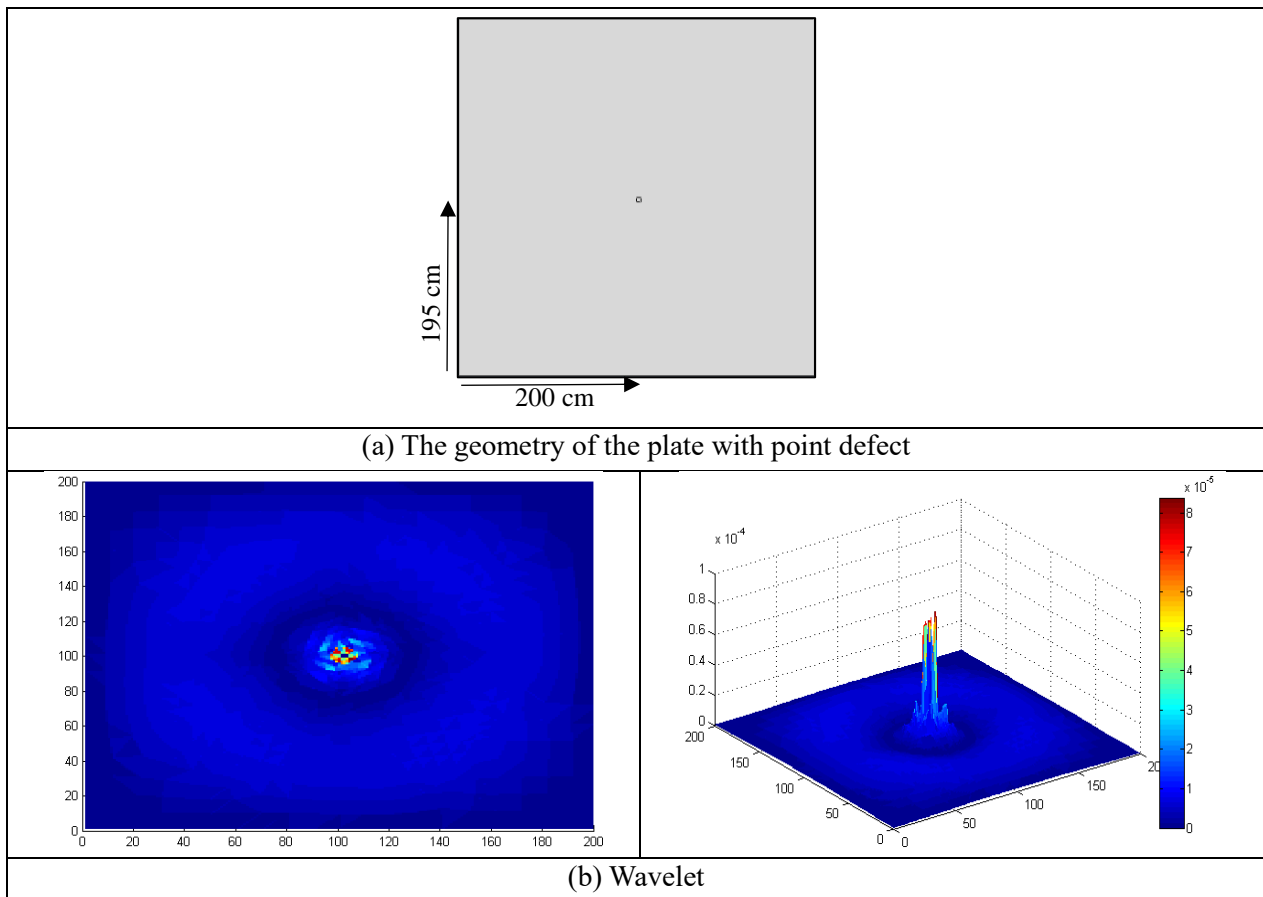
4.1. Numerical results

This research aims to present a new approach via shearlet transform compared with the other transforms; the wavelet transforms, Laplacian pyramid transform, curvelet transform, and contourlet transform; to find defect types in plate structures. To this end, the ability of all

transforms to detect cracks of plate structures was evaluated with eight numerical examples. In all cases, a square plate with a thickness of 10 cm was considered with four fixed boundary conditions. Properties of plate material included Young's modulus of $E = 20 \text{ GPa}$, the mass density $\rho = 2500 \text{ kg/m}^3$, and Poisson's ratio of $\nu = 0.2$. It is worth mentioning that for simulating different geometry defects in the ABAQUS software, after modeling a plate, the defect with different shapes was considered in the plate as a new section with various materials. Then, all the plate could have meshed as one unit. The next step includes gathering results of ABAQUS such as nodal coordinates (x and y), and displacement in the y direction for the damaged and undamaged plates. In MATLAB software; these four vectors are considered input variables. In this step, the scatter interpolate method has been used to make a mesh grid in the x and y directions.

4.1.1. The plate with a point defect

The first example contains a plate with a width of 400 cm and a length of 400 cm, including a square point damage with 5 cm length and width, located as shown in Fig. 8.



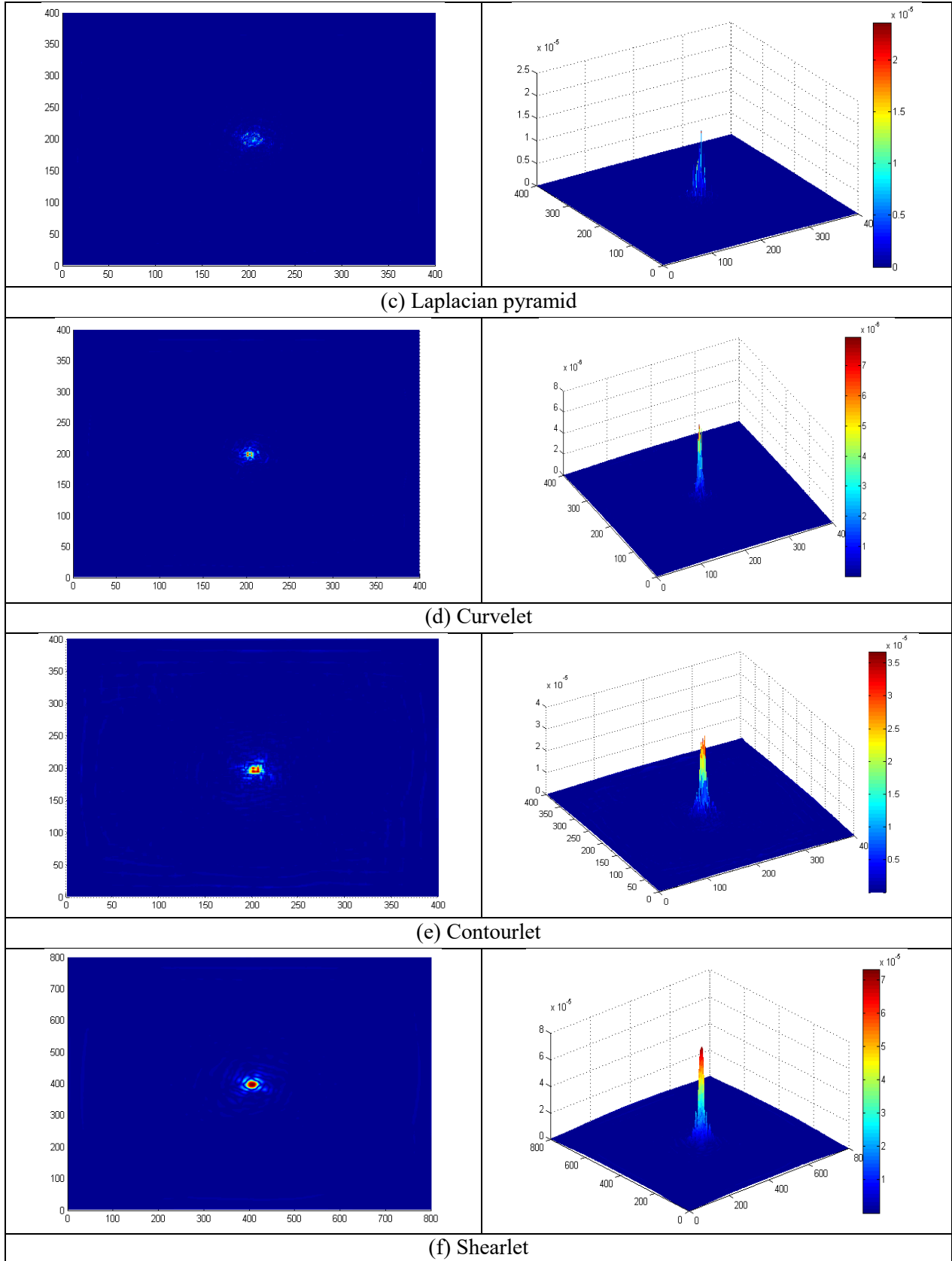
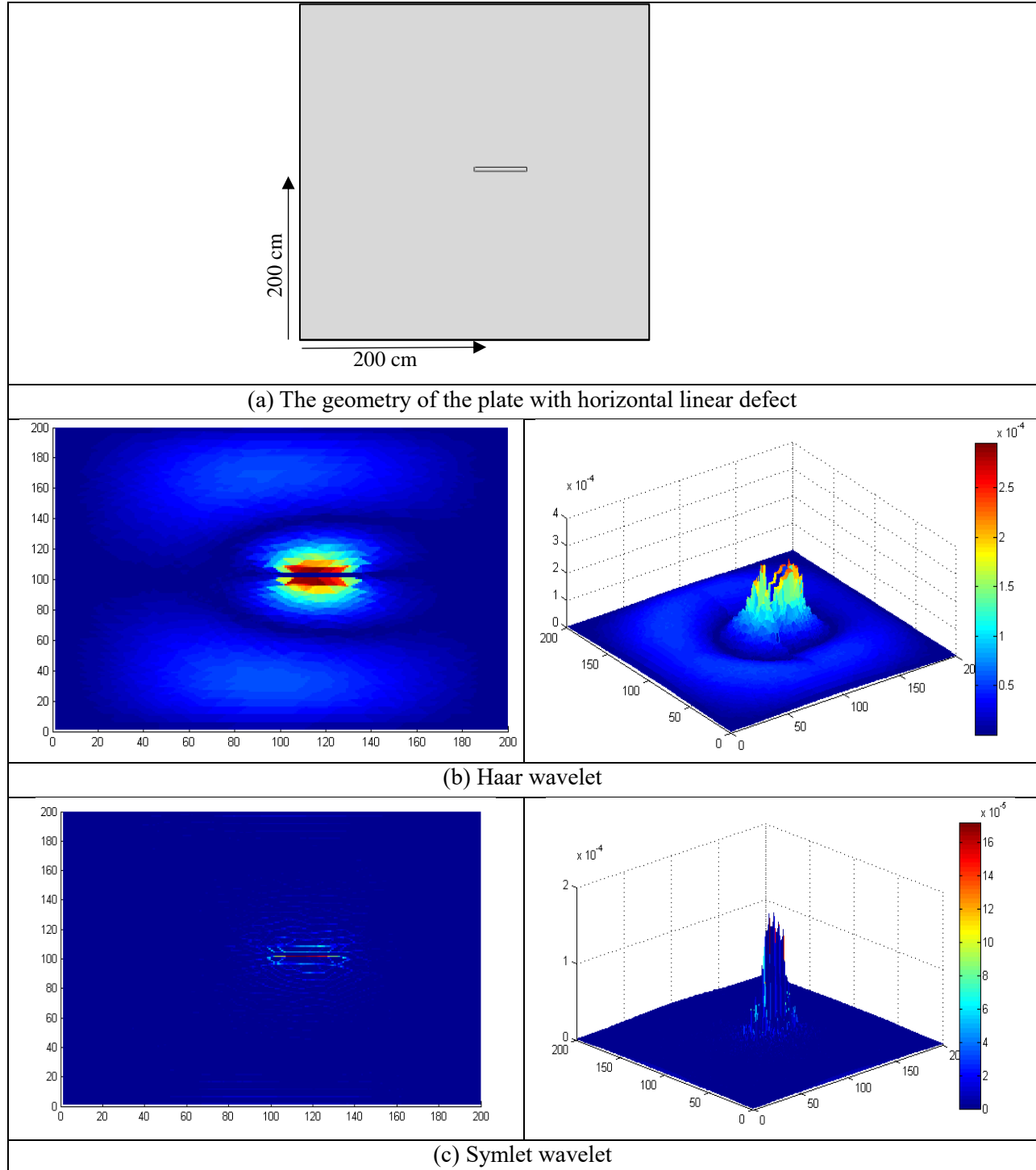
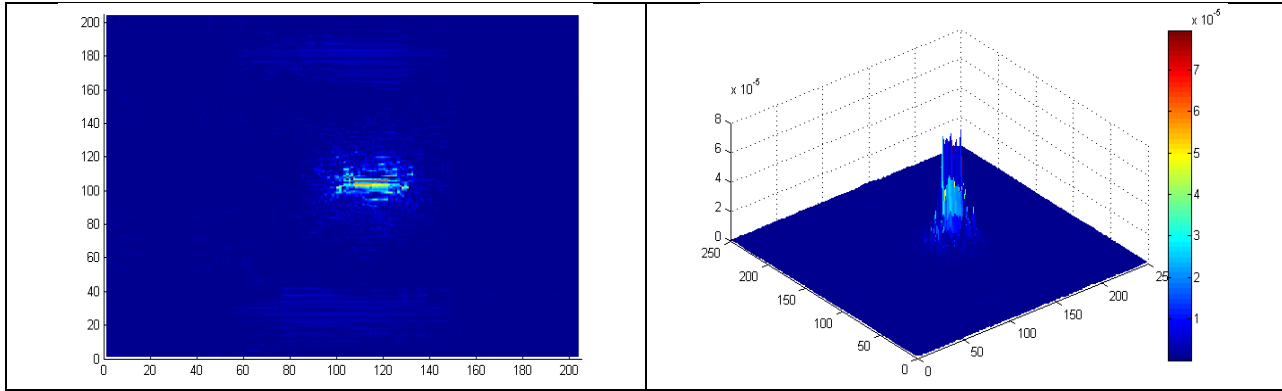


Fig. 8. Point damage detection.

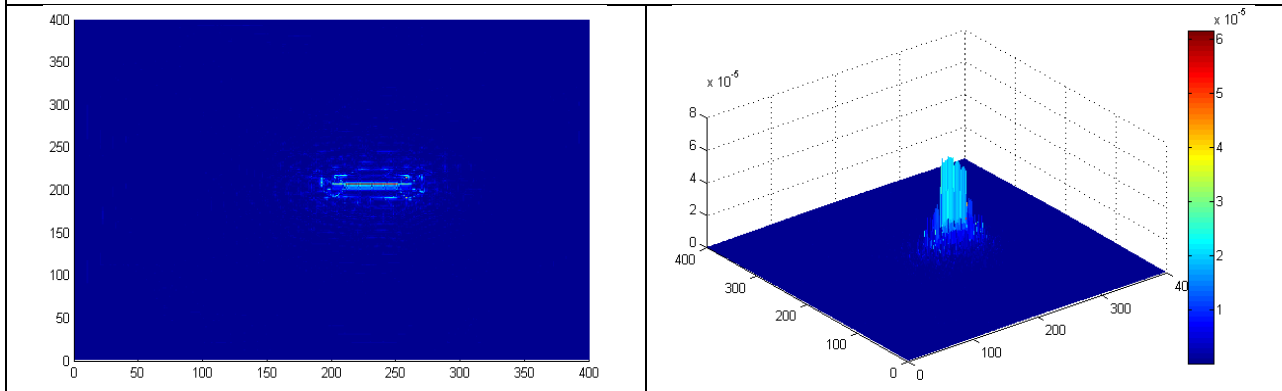
4.1.2. The plate with a horizontal linear defect

The second example includes a plate with a width of 400 cm and a length of 400 cm, containing a horizontal linear defect with 60 cm length and 5 cm width, which is located as illustrated in Fig. 9.

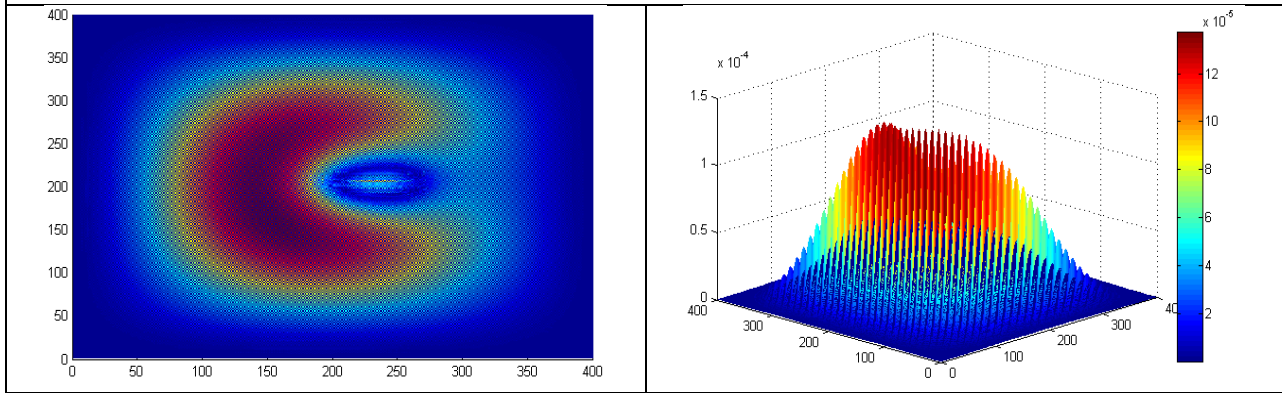




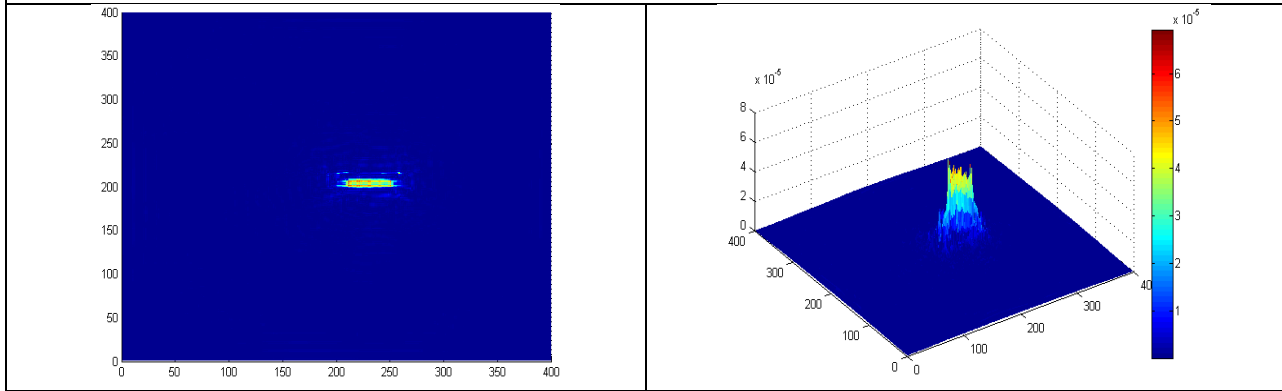
(d) Discrete Meyer wavelet



(e) Laplacian pyramid (9/7 filter)



(f) Laplacian pyramid (PKVA filter)



(g) Curvelet

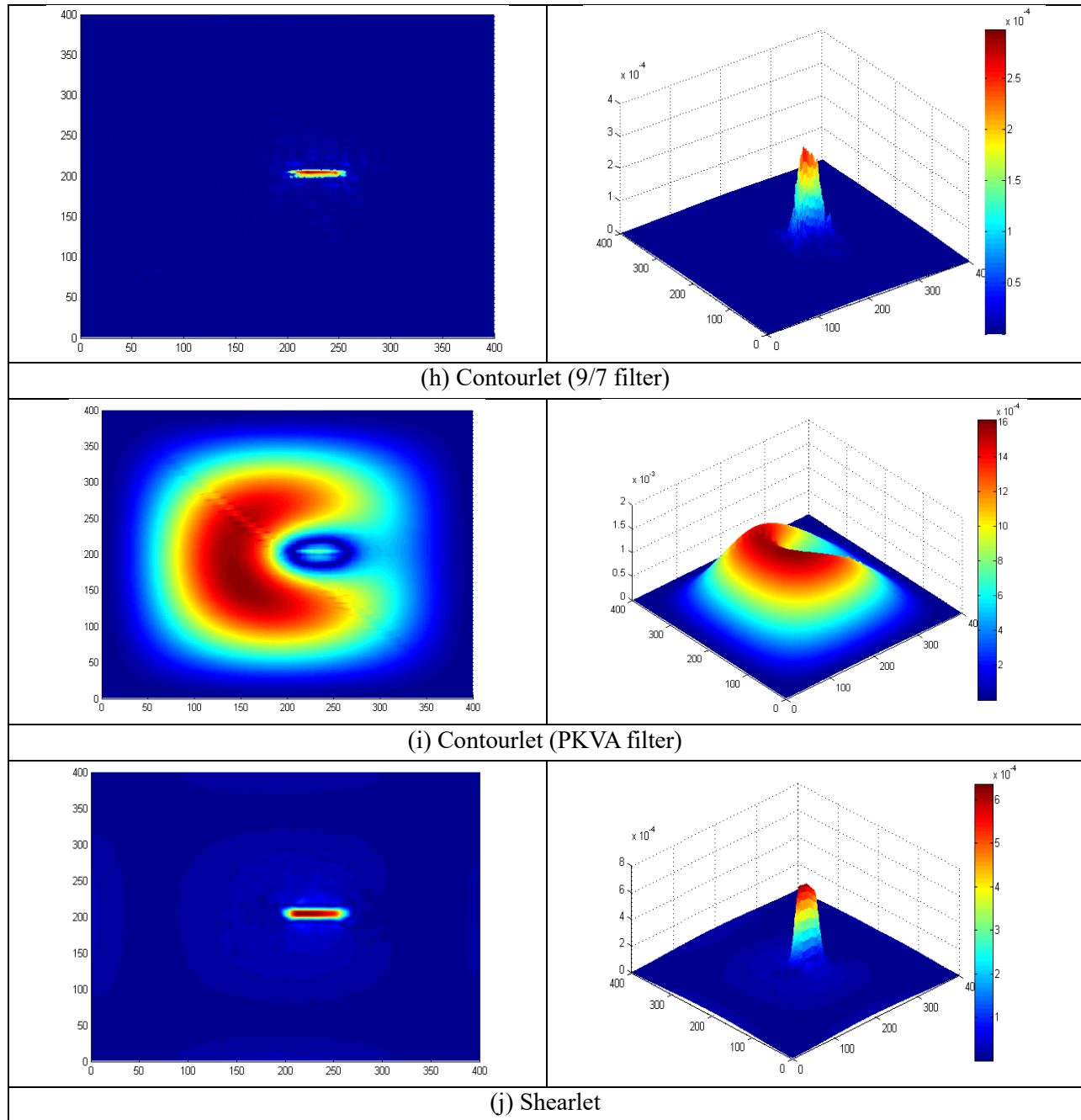
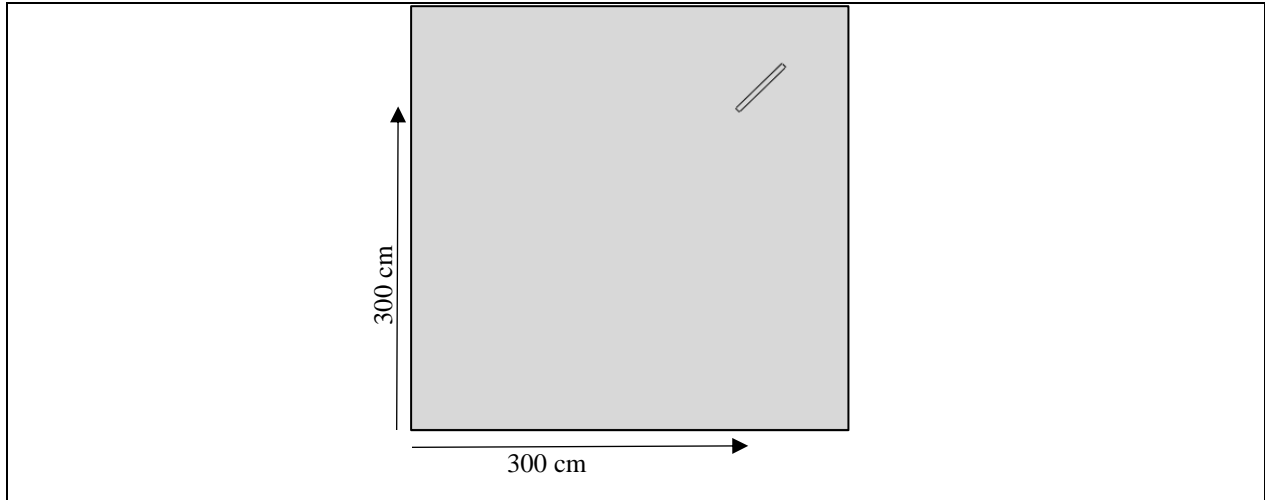


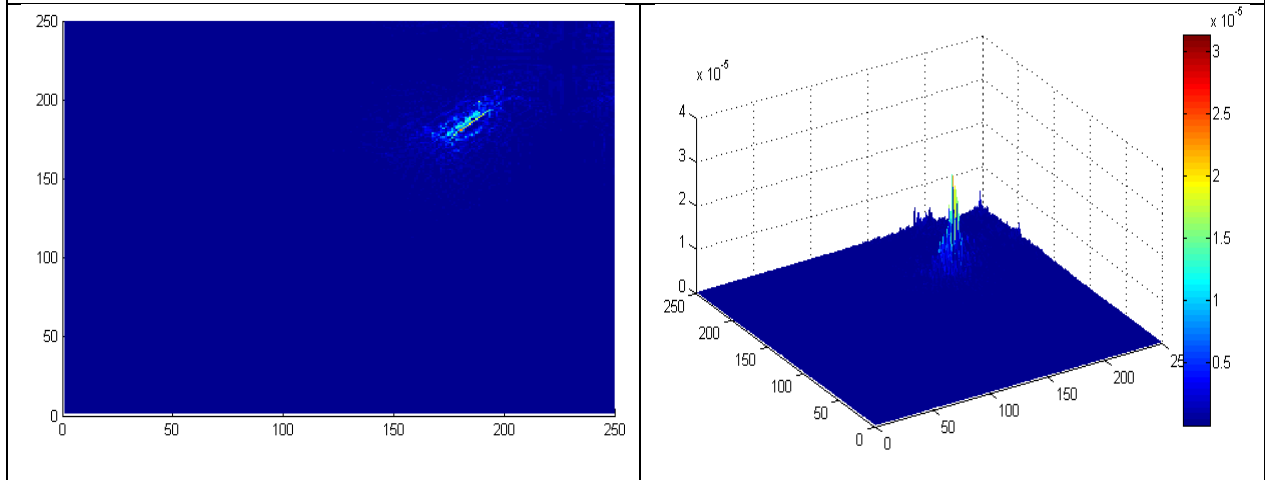
Fig. 9. Horizontal linear damage detection.

4.1.3. The plate with a diagonal linear defect

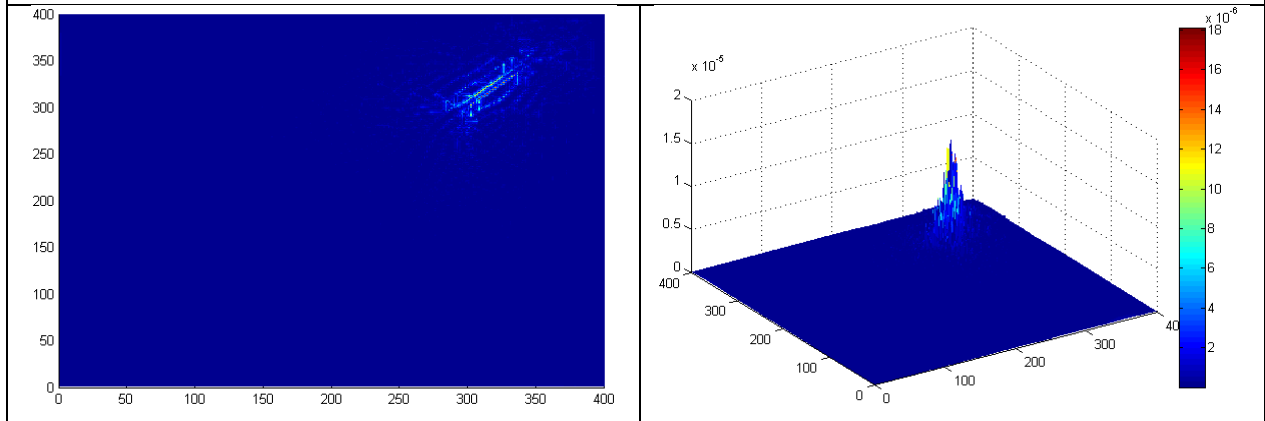
The third example consists of a fixed support plate with a width of 400 cm and a length of 400 cm, including a diagonal linear damage with 60 cm length, 5 cm width, and the angle of 45° located as in Fig. 10.



(a) The geometry of the plate with a diagonal linear defect



(b) Discrete Meyer wavelet



(c) Laplacian pyramid (9/7 filter)

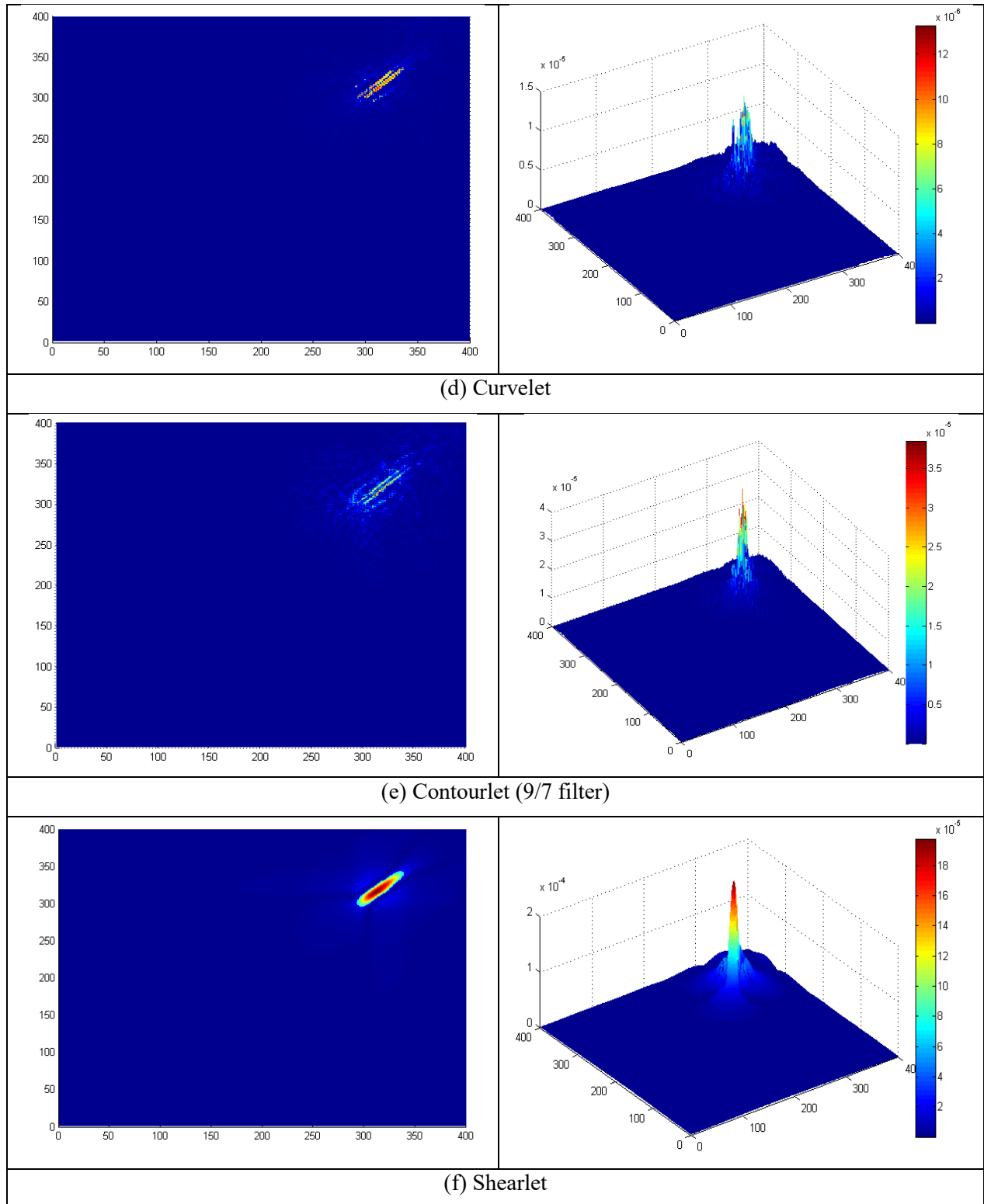
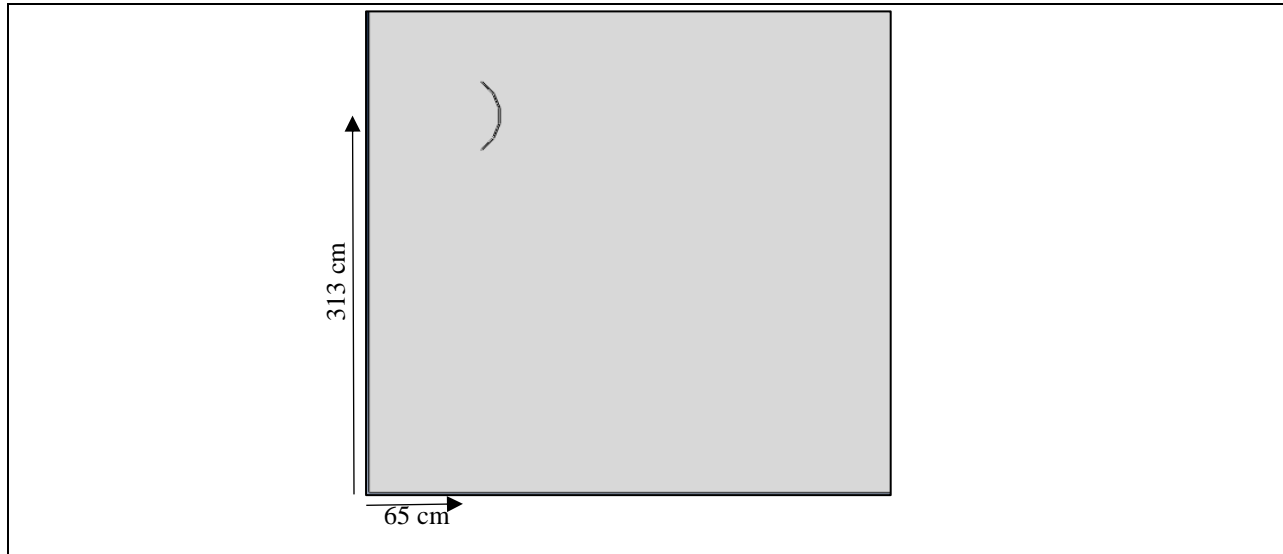


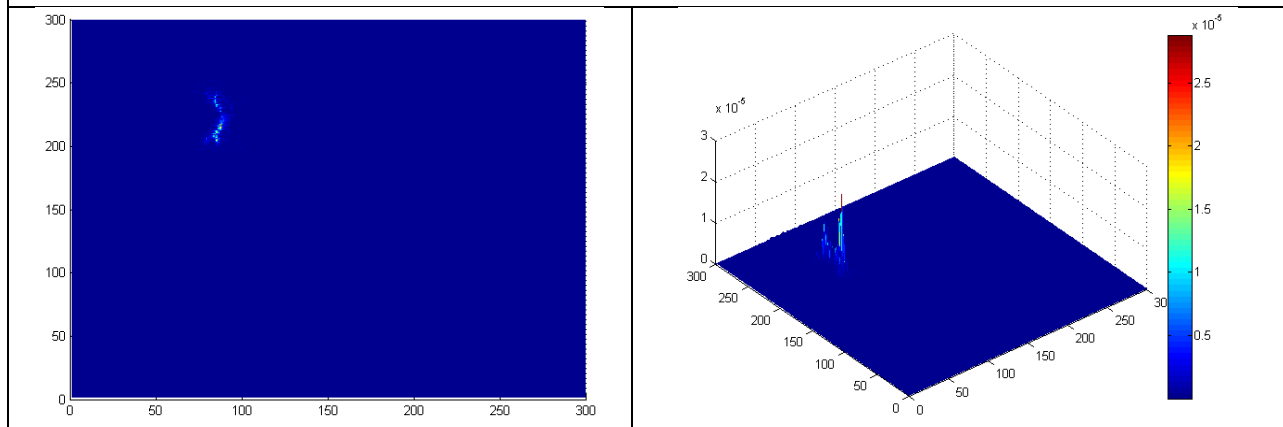
Fig. 10. Diagonal linear damage detection.

4.1.4. The plate with an arc defect

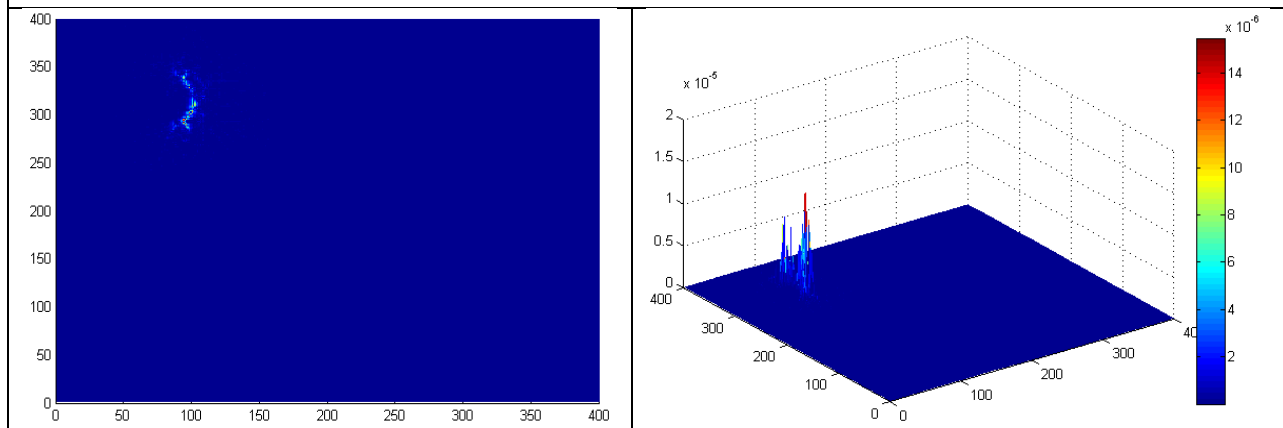
The fourth example comprises a fixed support plate with a width of 400 cm and a length of 400 cm, containing a curved defect with 66 cm length and 1 cm width, and coordinates of the arc center are as shown in Fig. 11.



(a) The geometry of the plate with arc defect



(b) Discrete Meyer wavelet



(c) Laplacian pyramid (9/7 filter)

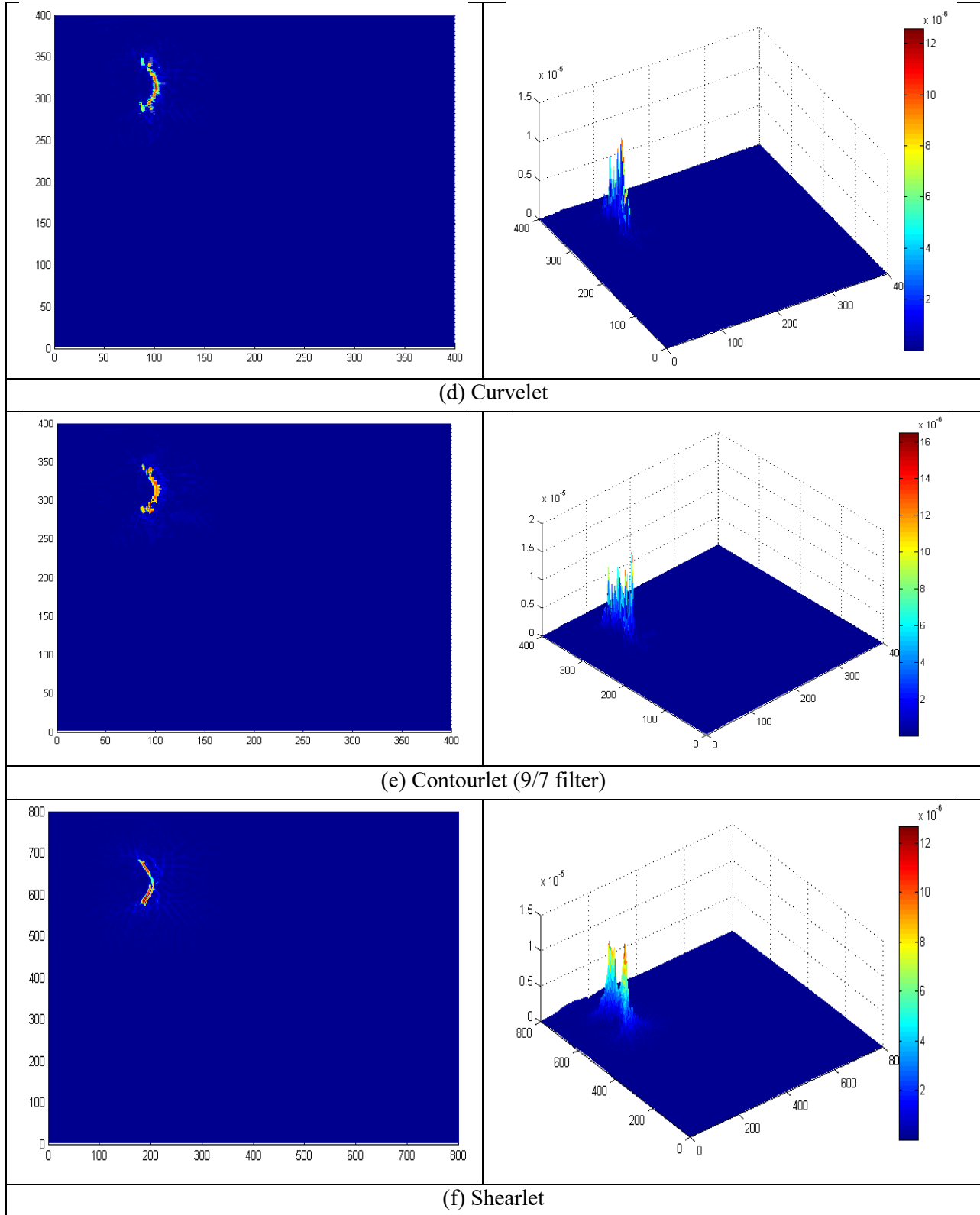
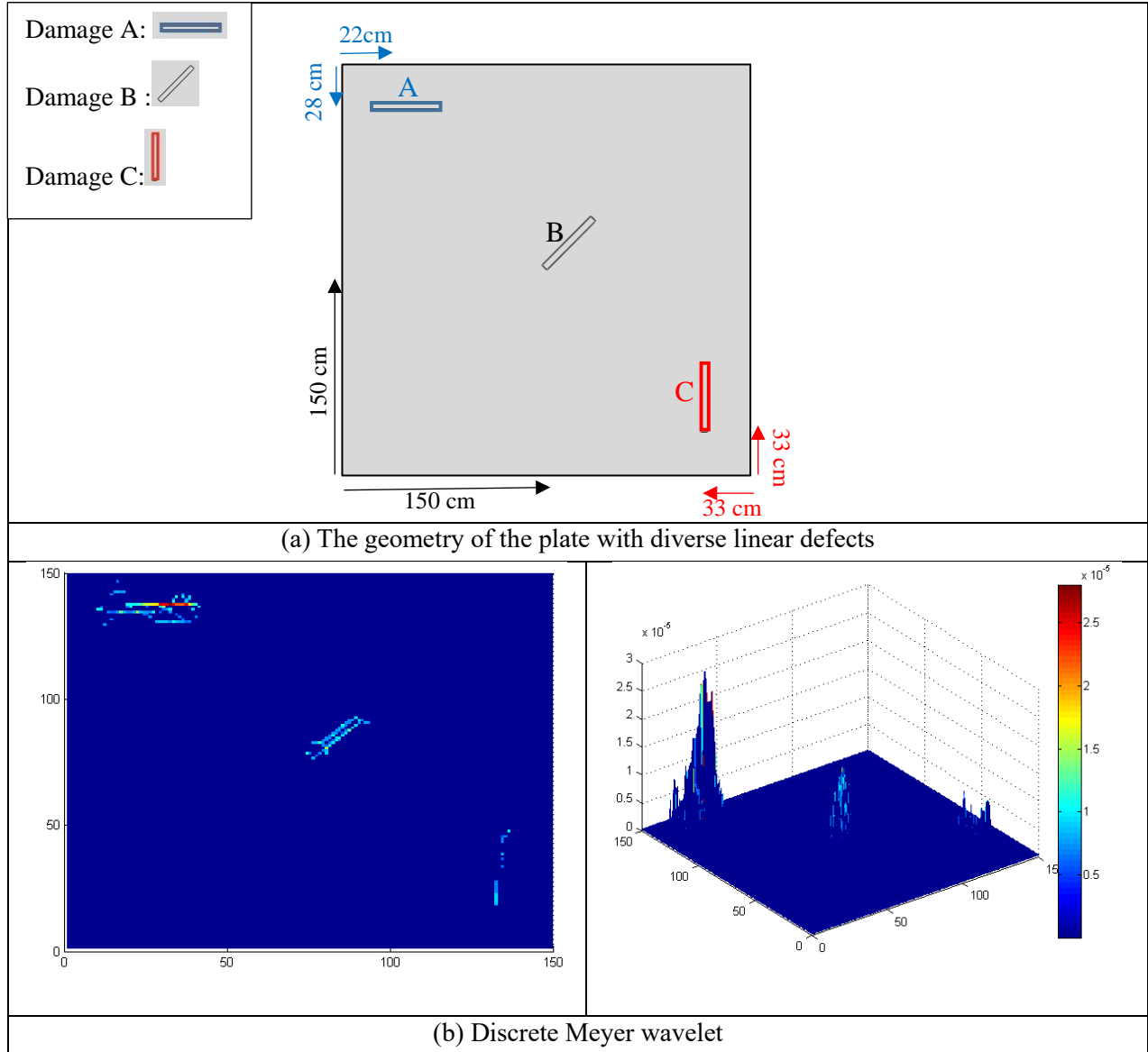
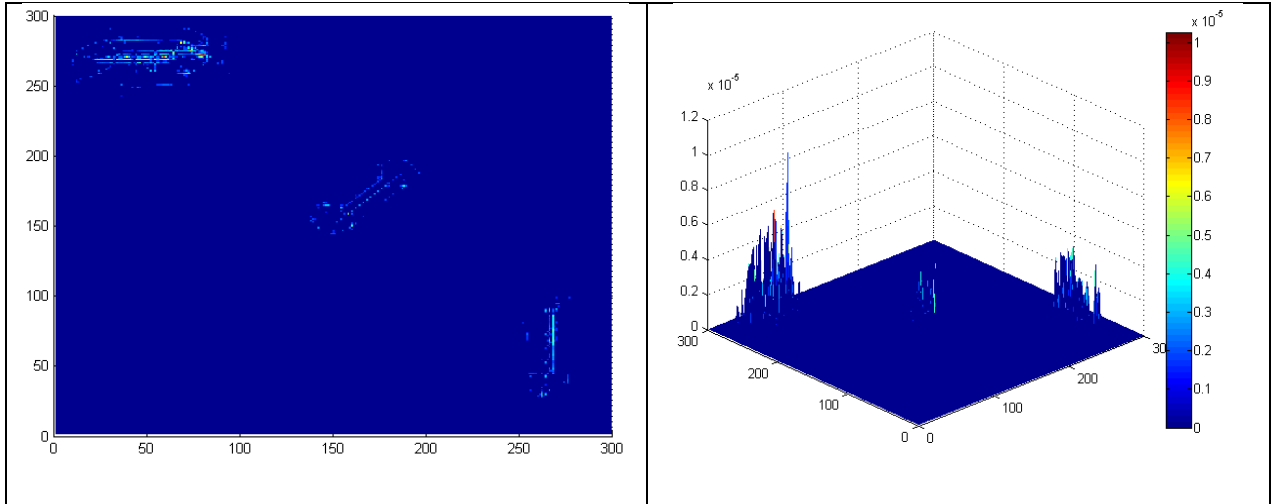


Fig. 11. Arc damage detection.

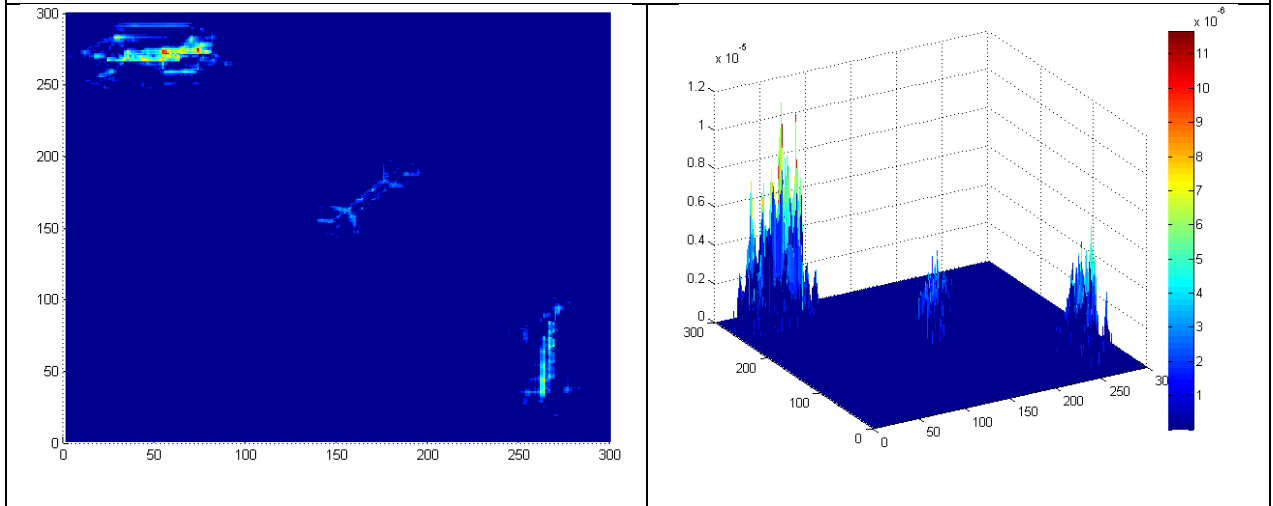
4.1.5. The plate with diverse linear defects

The fifth example includes a fixed support plate with a width of 300 cm, length of 300 cm, and three linear damages, including horizontal, vertical, and diagonal. The size of the defects is as follows: 60 cm length and 5 cm width; the diagonal linear defect with the angle of 30°. The location of these defects is depicted in Fig. 12.

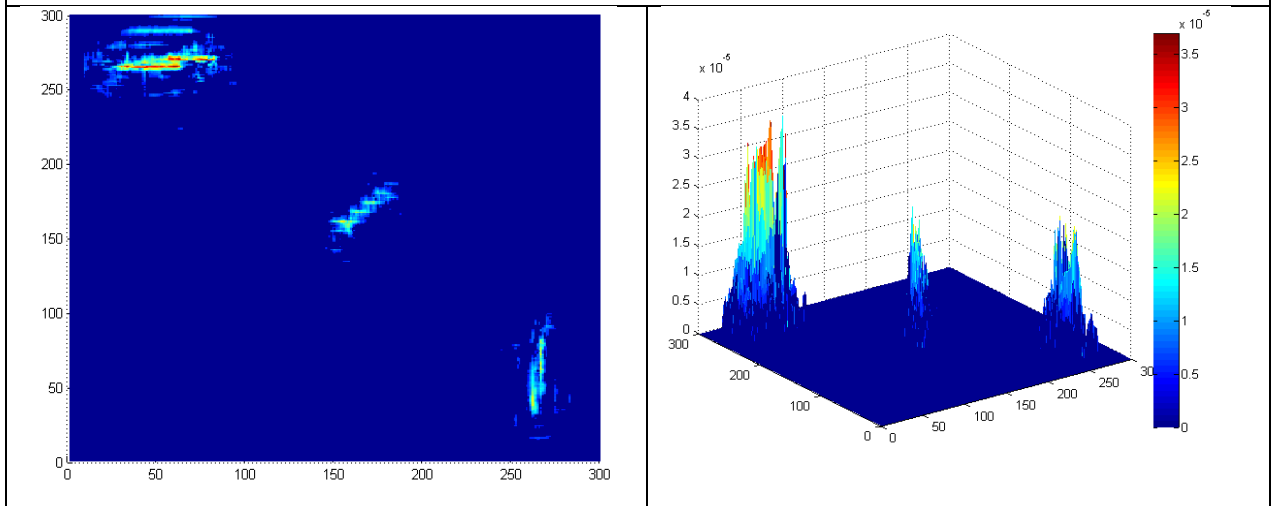




(c) Laplacian pyramid (9/7 filter)



(d) Curvelet



(e) Contourlet (9/7 filter)

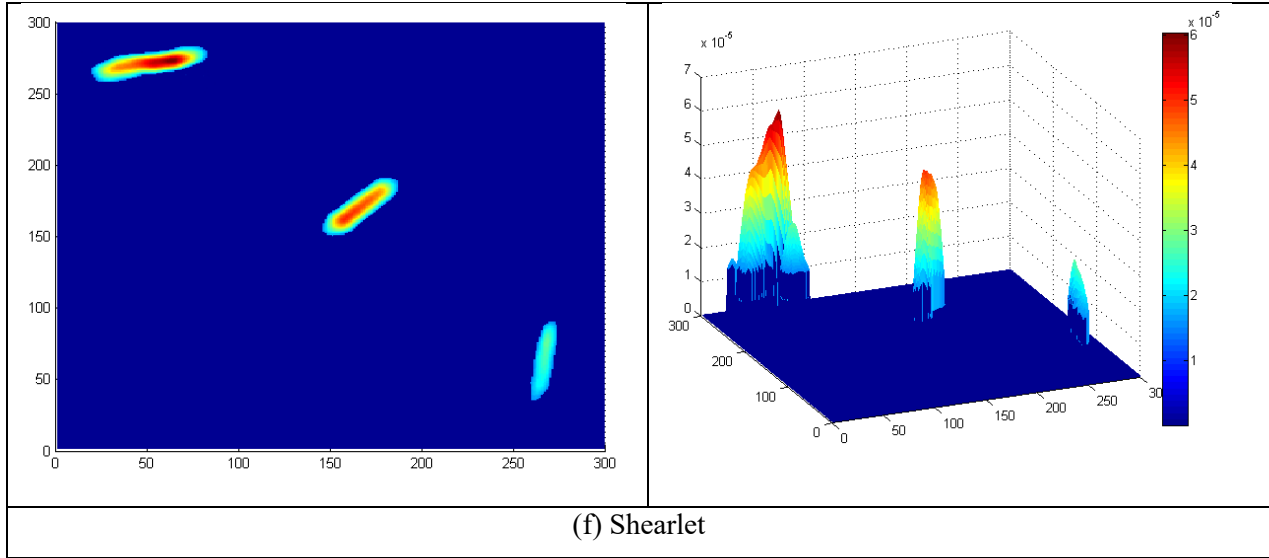
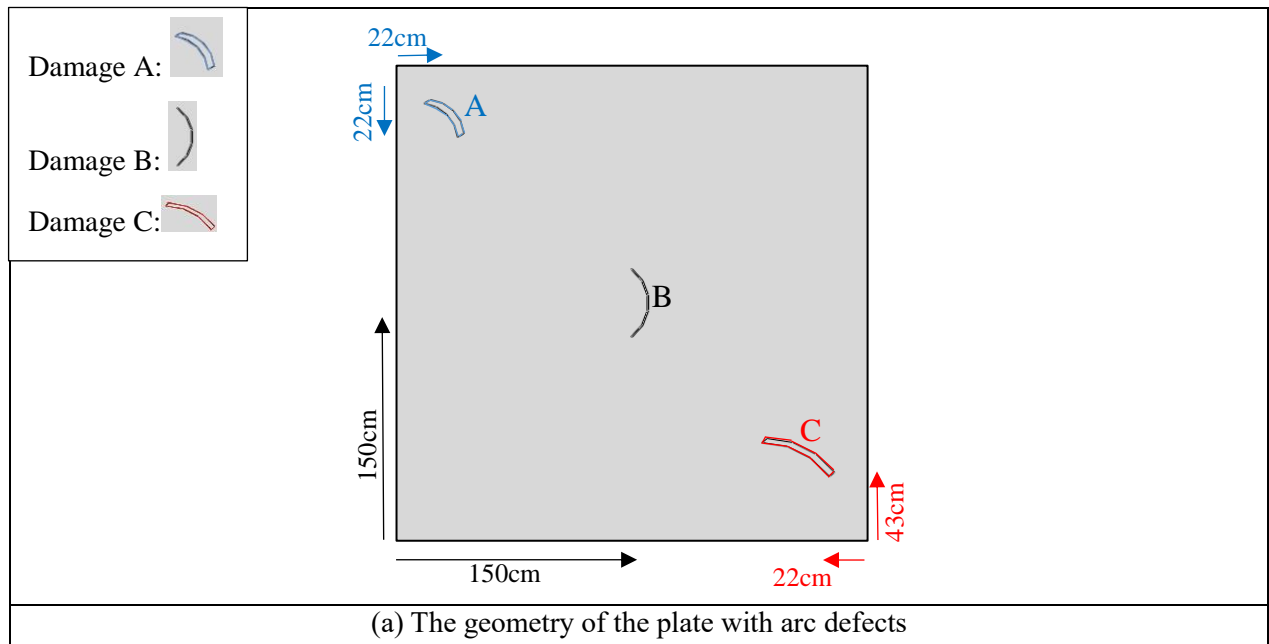
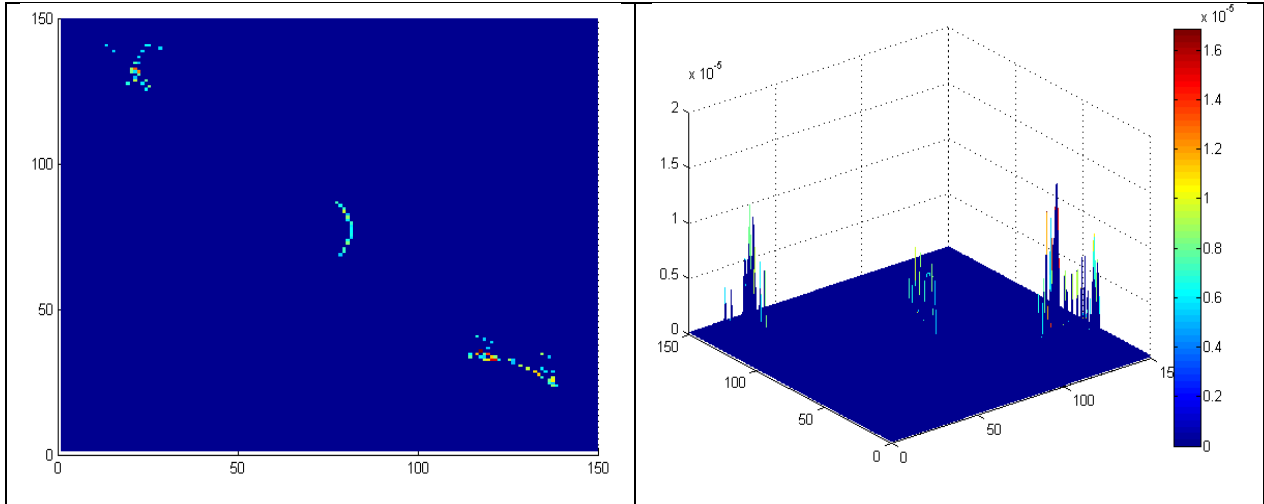


Fig. 12. Diverse linear damages detection.

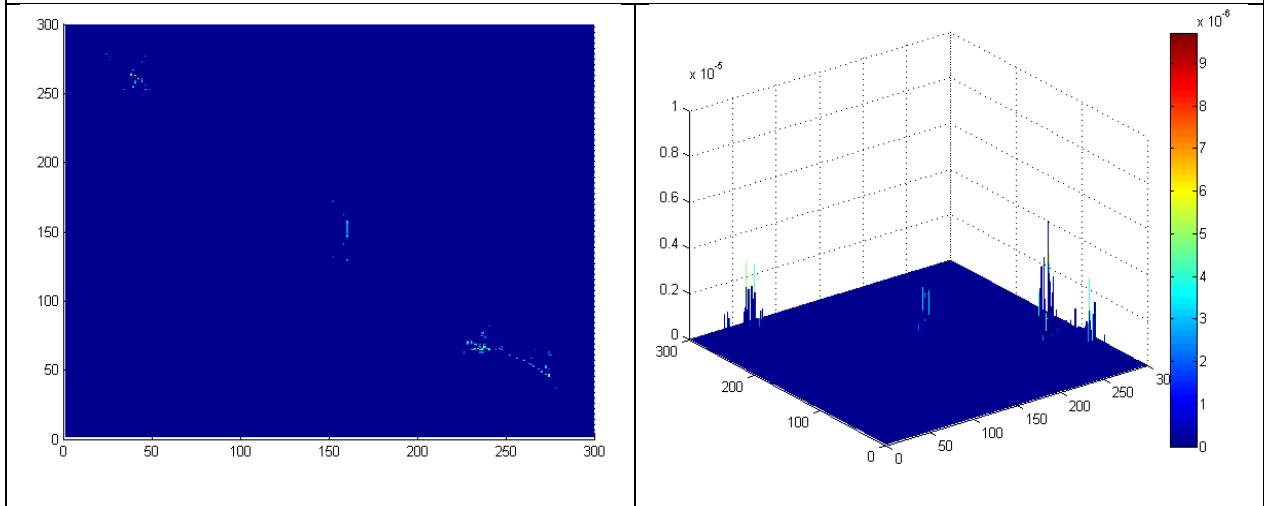
4.1.6. The square plate with arc defects

The sixth example includes a fixed support plate with a width of 300 cm, length of 300 cm, and three curved defects. The sizes of these defects are as follows: curve damage A with a length of 31 cm and width of 4 cm; curve damage B with the length of 50 cm and width of 1 cm; curve damage C with the length of 50 cm and width of 4 cm. The locations of these defects are shown in Fig. 13.

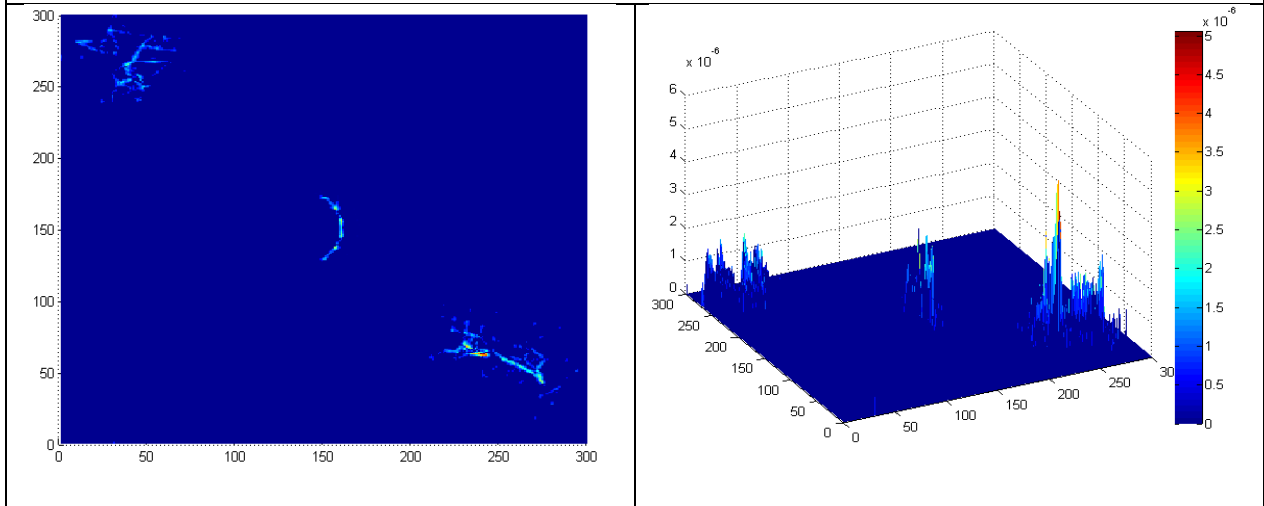




(b) Discrete Meyer wavelet



(c) Laplacian pyramid (9/7 filter)



(d) Curvelet

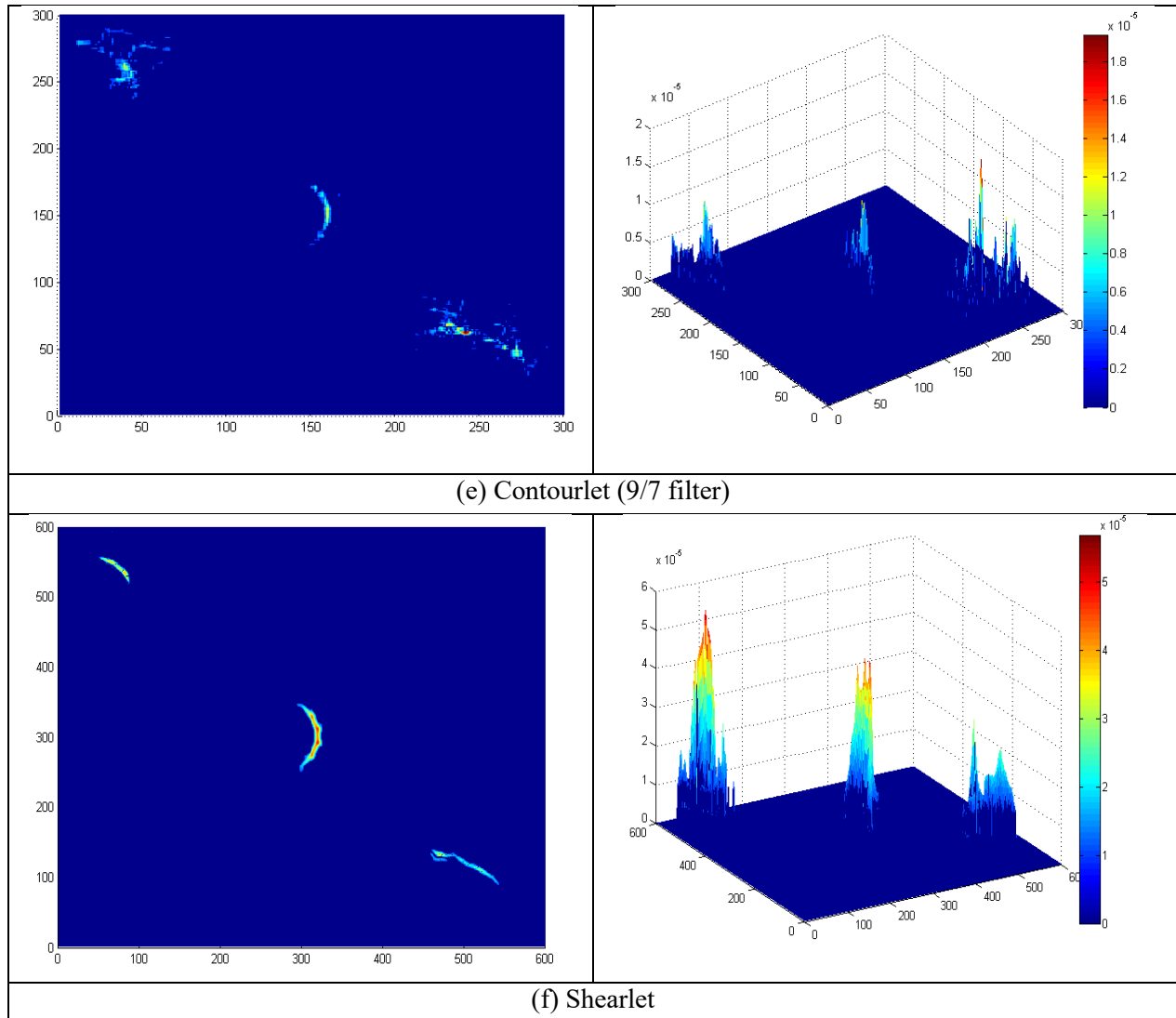
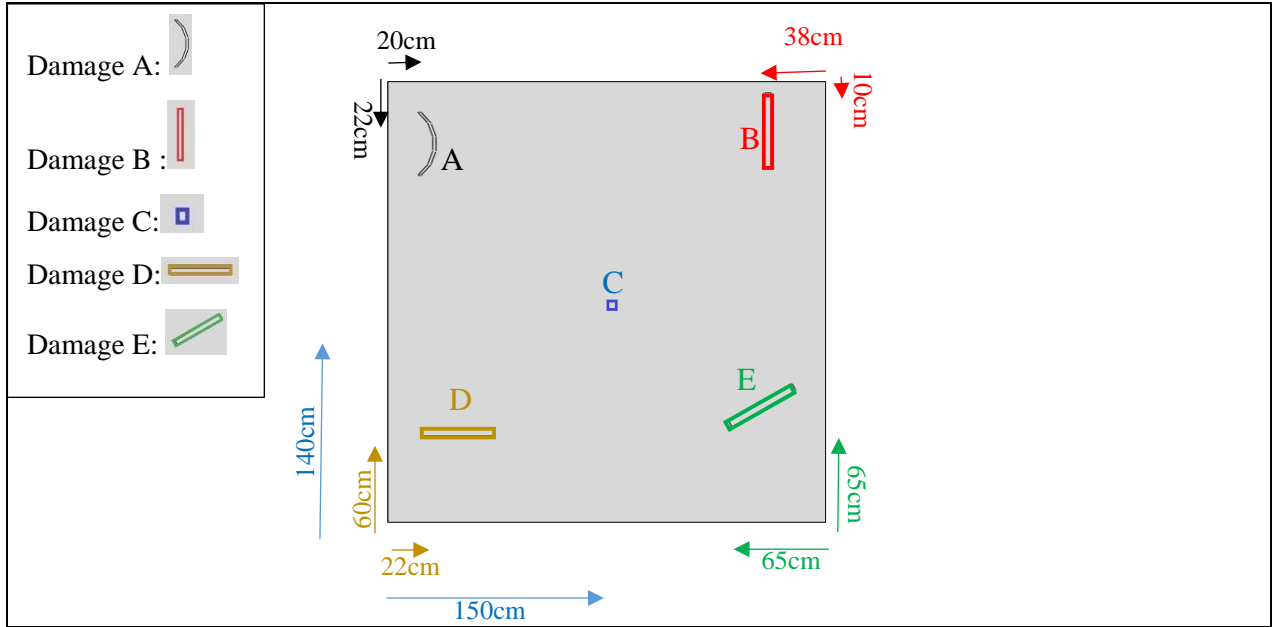


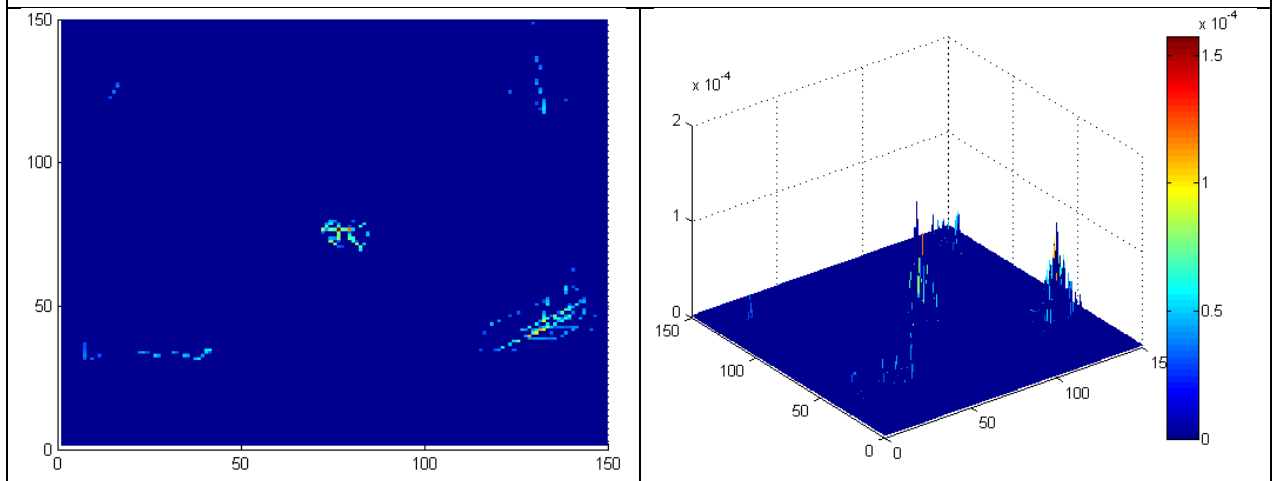
Fig. 13. Arc damage detection.

4.1.7. The plate with five diverse defects

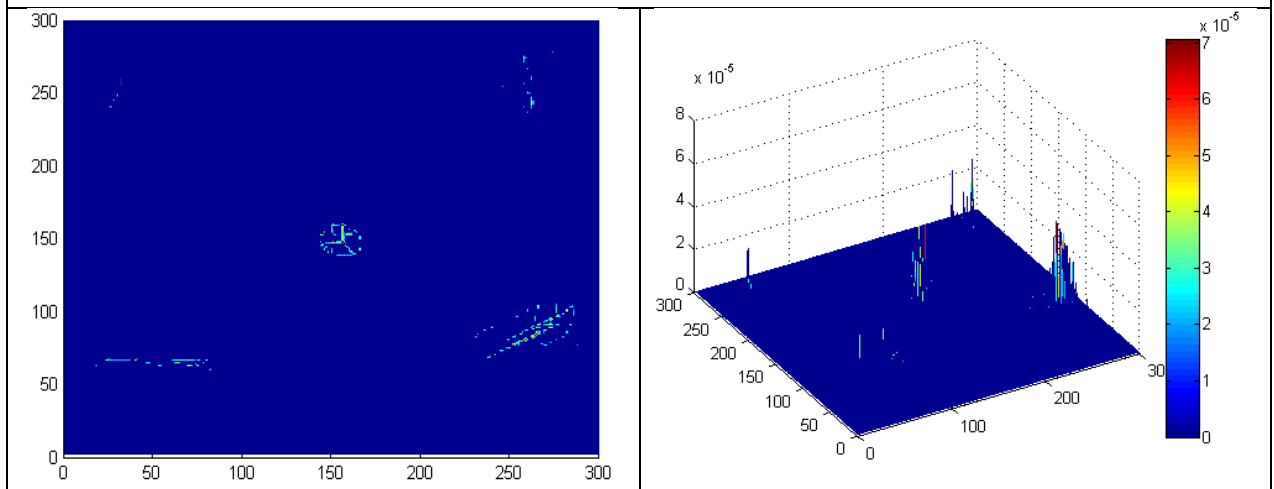
The seventh example includes a plate with a width of 300 *cm* and a length of 300 *cm*, which contained five defects. The linear defects (horizontal, vertical, and diagonal) have a length of 50 *cm* and width of 5 *cm*, and the diagonal linear defect with an angle of 30°. Also, the curve damage has a length of 48 *cm* and width of 2 *cm*, and dimensions of the square defect are 5 *cm*. The locations of these defects are indicated in Fig. 14.



(a) The geometry of the plate with five diverse defects.



(b) Discrete Meyer wavelet



(c) Laplacian Pyramid (9/7 filter)

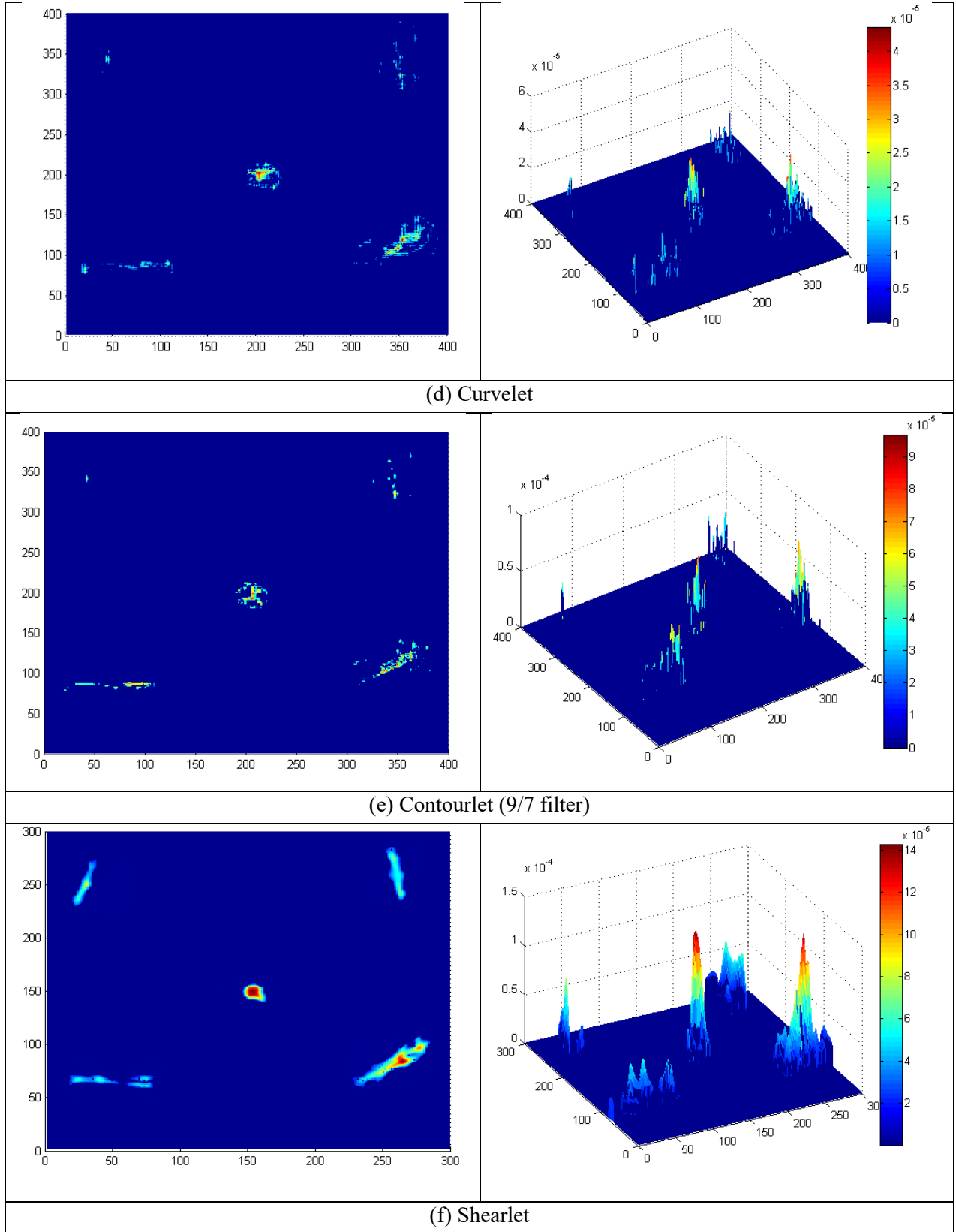
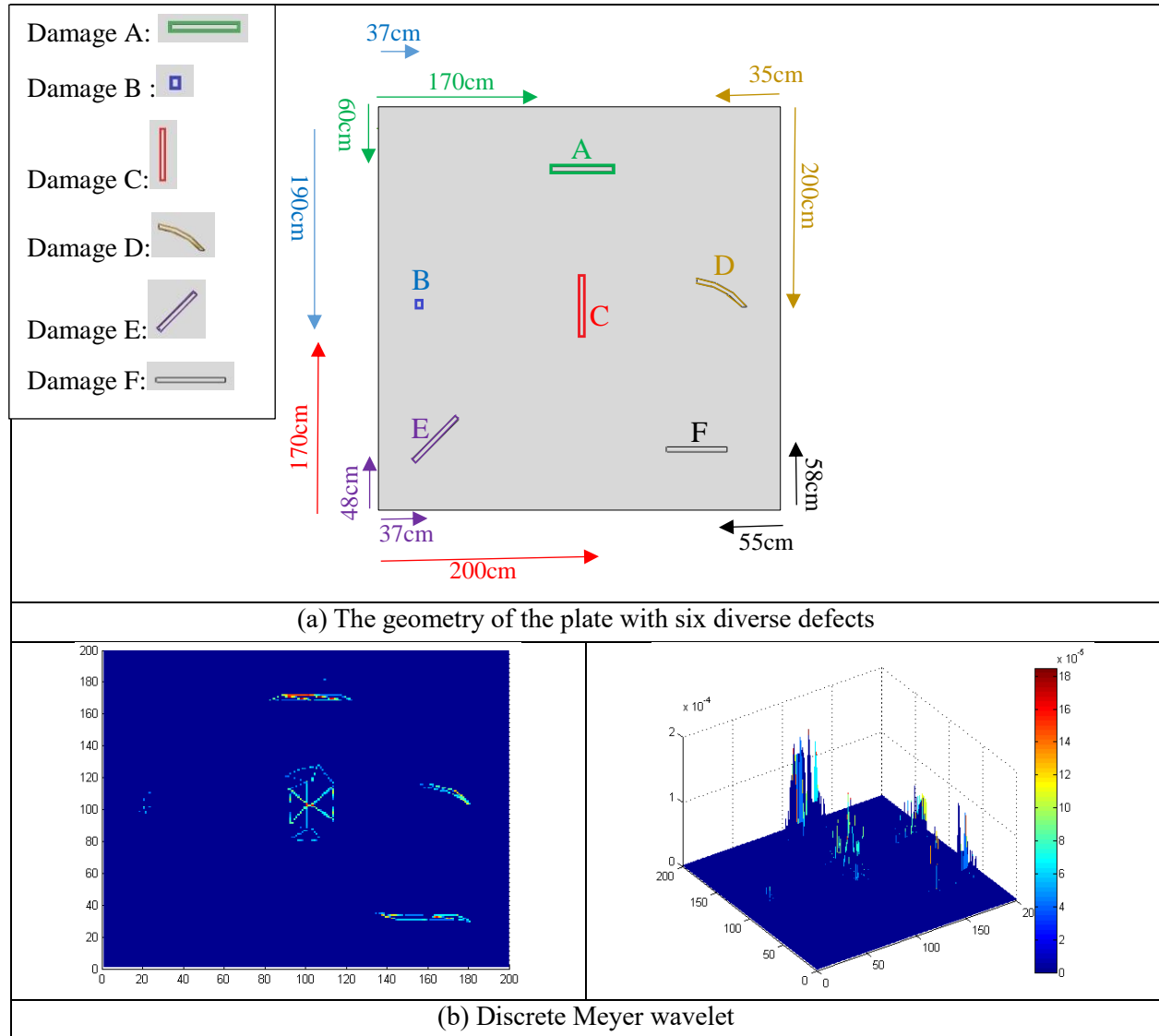


Fig. 14. Five diverse defects detection.

4.1.8. The plate with six diverse defects

The eighth example includes a plate with a width of 400 cm and a length of 400 cm containing six defects. The linear defects (horizontal, vertical, and diagonal) have a length of 60 cm and a width of 5 cm, and the diagonal linear defect with the angle of 45°. Also, the curve damage has a length of 50 cm and width of 5 cm, and square defect dimensions are 7 cm. The locations of these defects are displayed in Fig. 15.



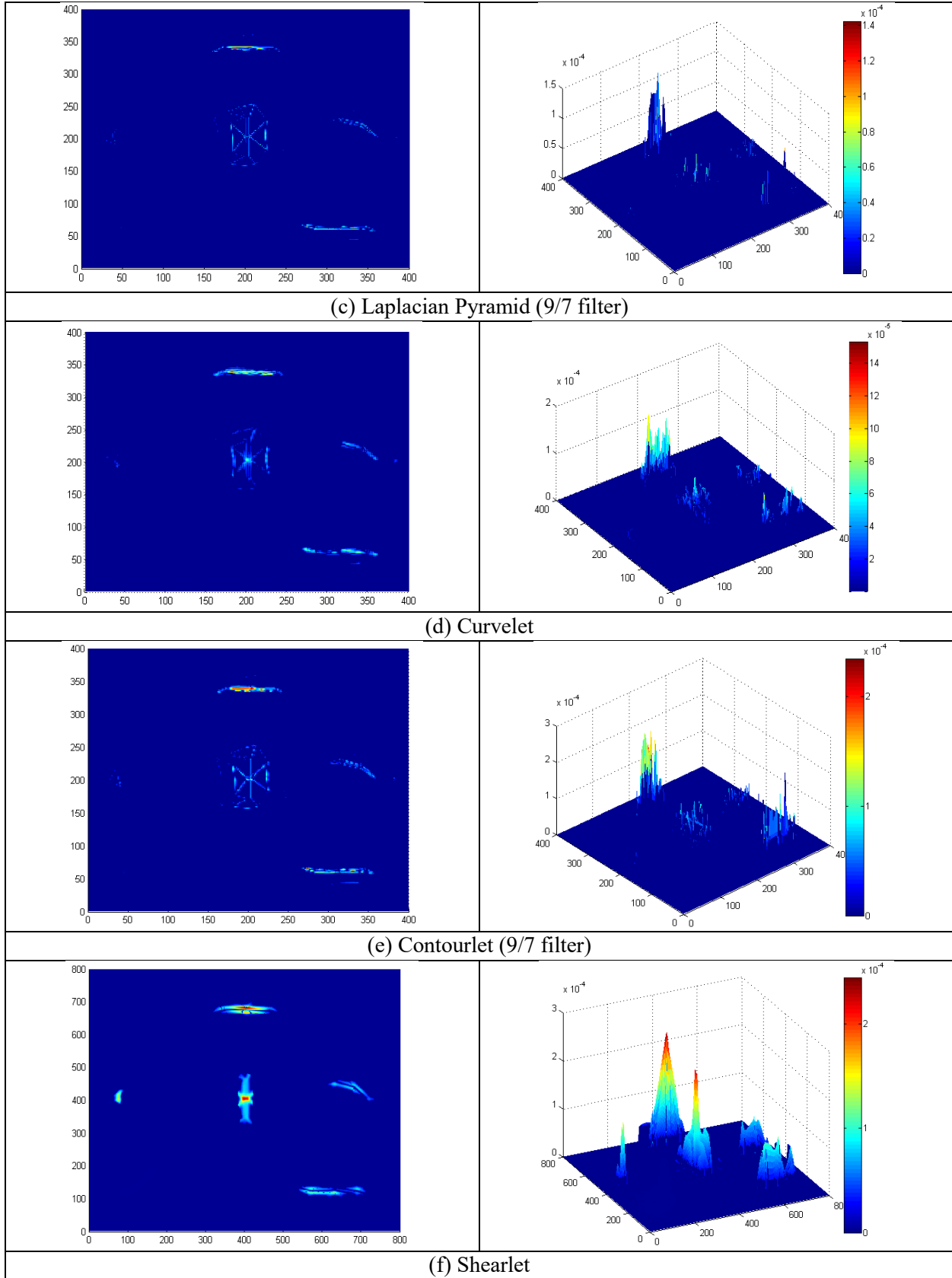
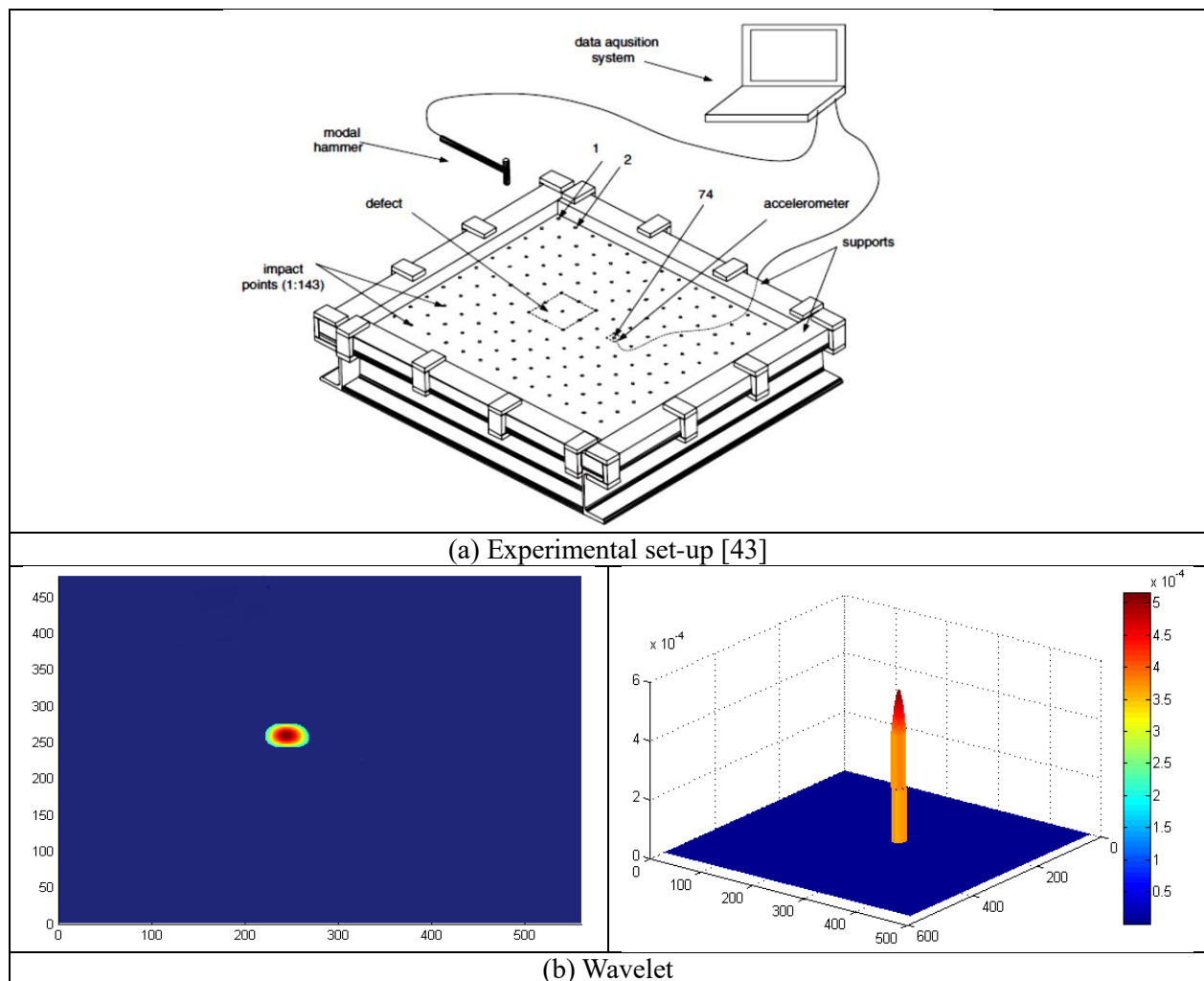


Fig. 15. Six diverse defects detection.

4.2. Experimental validation

In this section, the capabilities of the transforms (wavelet, Laplacian pyramid, contourlet, curvelet, and shearlet) were evaluated using the vibration response data of a steel plate proposed by Rucka and Wilde [43]. It is worth mentioning that the data from Rucka and Wilde's paper is not publicly available. Also, the experimental data includes the undamaged state exclusively; hence, the damaged state was attained numerically. In addition, using experimental data has some problems such as lack of all measured DOFs and incomplete modal data; see these references for more information [44–46]. Fig. 16 depicts the steel plate with the length of $L = 560\text{ mm}$, width of $B = 480\text{ mm}$, and height of $H = 2\text{ mm}$. The plate Young's modulus, Poisson's ratio, and mass density were $E = 192\text{ GPa}$, $\nu = 0.25$, and $\rho = 7430\text{ kg/m}^3$, respectively. The plate included a rectangular defect with $L_d = 80\text{ mm}$, $B_d = 80\text{ mm}$, and $H_d = 0.5\text{ mm}$. The starting point of the damage was located at $x = 200\text{ mm}$ and $y = 200\text{ mm}$. The transforms are applied to the fundamental mode shape to identify faults. Also, data de-noising was carried out based on the process in section of de-noise the structural response of the plates.



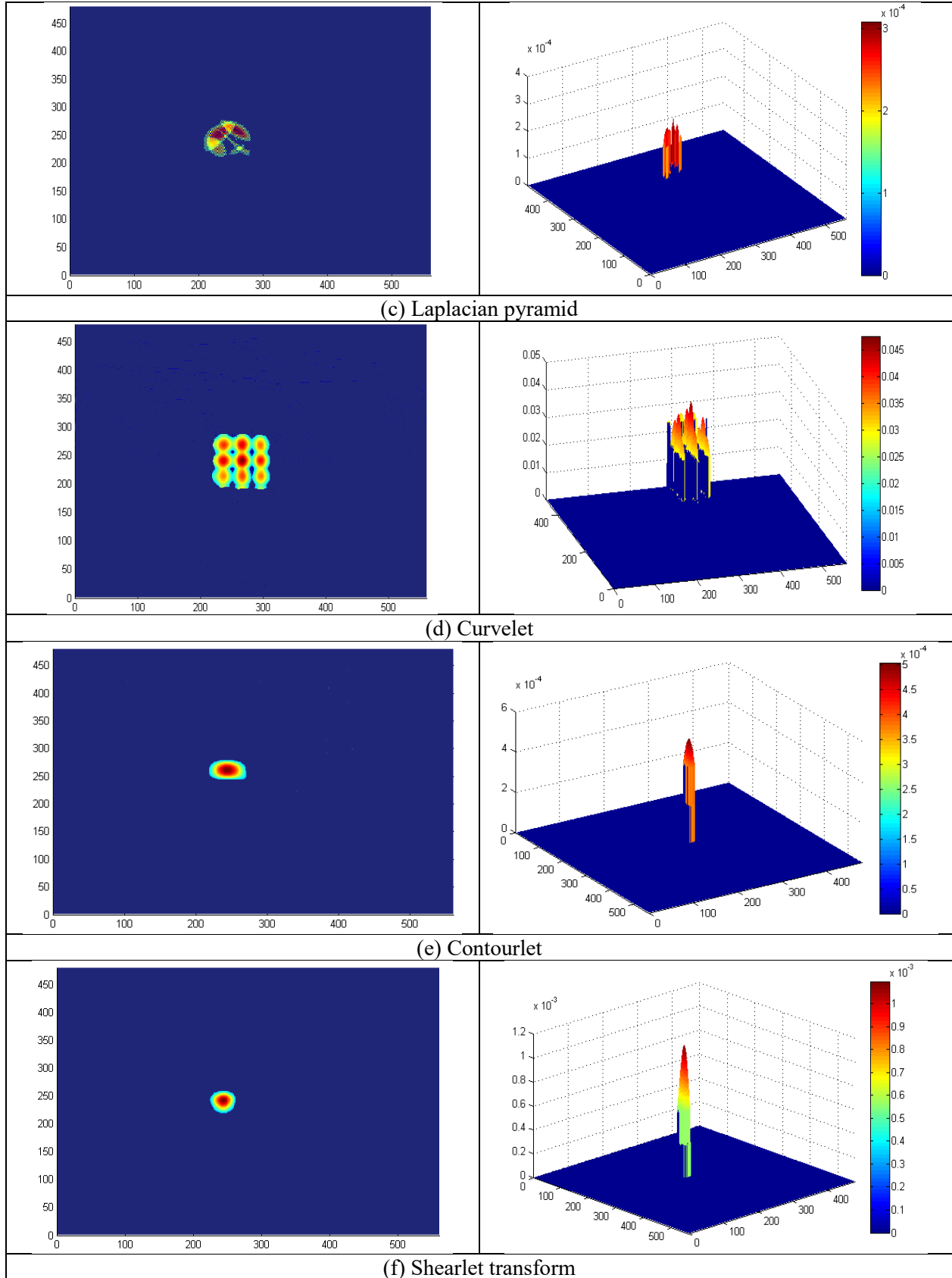
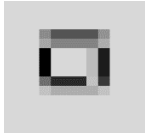
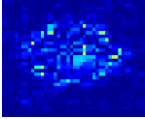
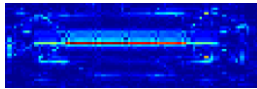
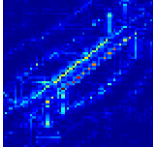
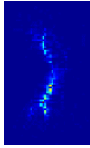
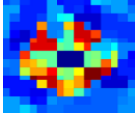
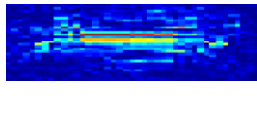
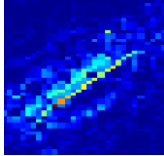
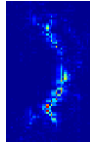
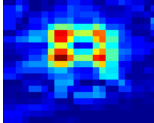
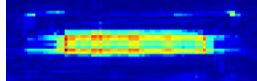
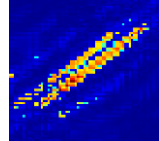
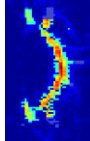
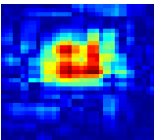
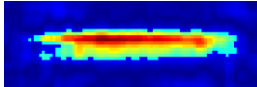
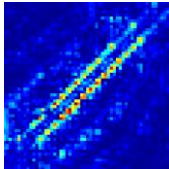
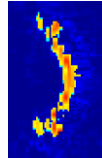
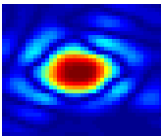
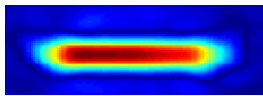
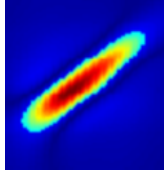
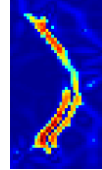


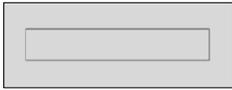
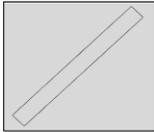
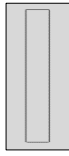
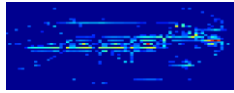
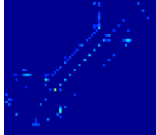
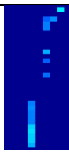
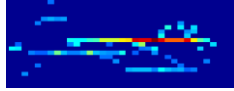
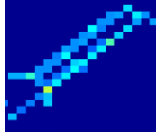
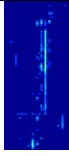
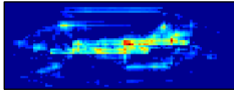
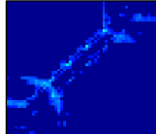
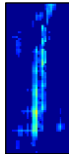
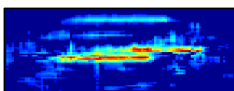
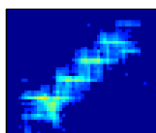
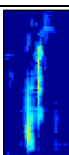
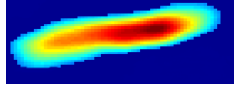
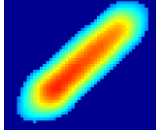
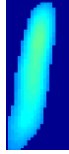
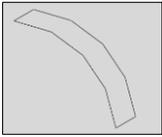
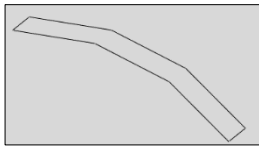
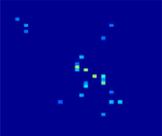
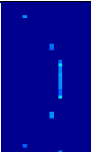
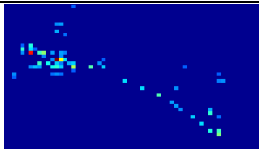
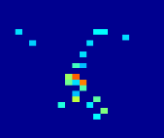
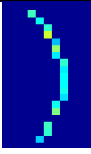
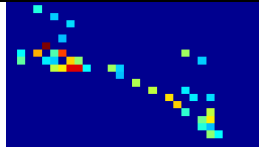
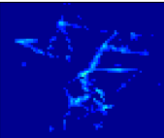
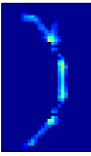
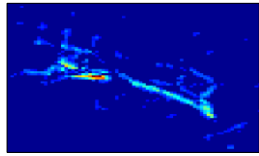
Fig. 16. Single experimental defect detection.

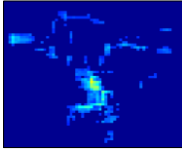
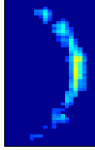
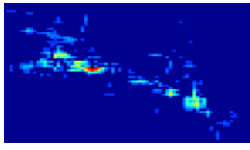
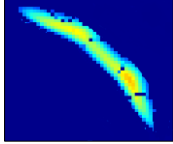
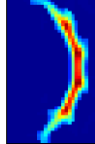
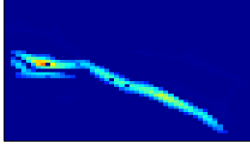
5. Discussion

In the following, the results of numerical and experimental examples are presented comprehensively (Fig. 17 demonstrates the overall summary of the numerical examples):

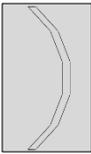
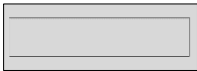
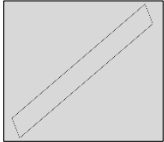
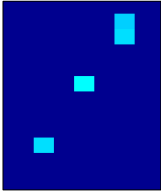
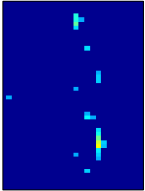
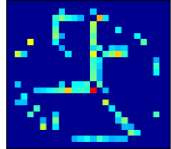
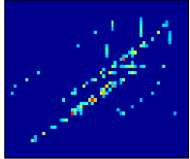
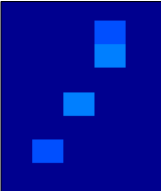
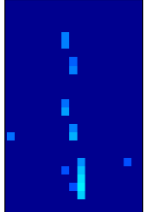
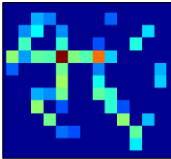
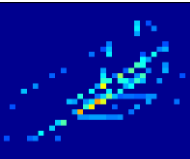
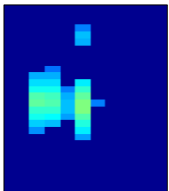
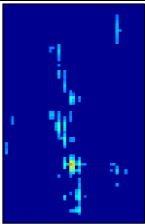
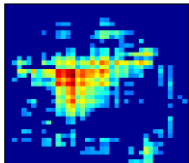
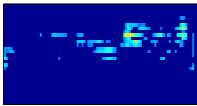
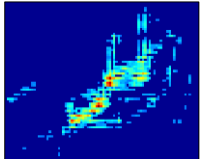
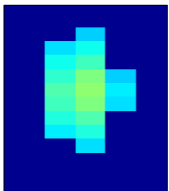
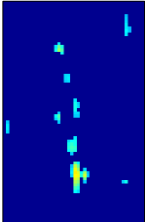
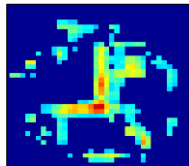
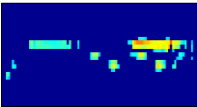
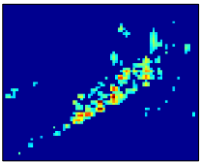
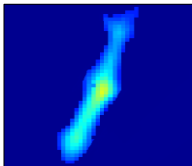
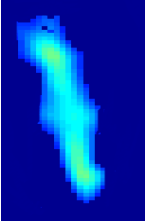
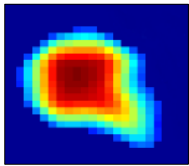
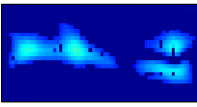
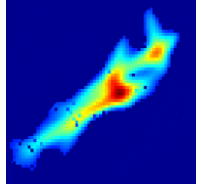
- The experimental results have displayed that the maximum values of damage index are located approximately at the place of the defect in all the transforms. Accordingly, the transforms—wavelet, Laplacian pyramid, curvelet, contourlet, and shearlet transform—can be adopted as applicable procedures to detect defects in all studies.
- To choose the proper wavelet based on the wavelet impact on fault demonstration, the ability of various wavelets— including Haar, Symlet, and Discrete Meyer wavelet – is evaluated in the second example. As the shape of the horizontal linear defect is more vivid in the Discrete Meyer wavelet demonstration. Hence, damage presentation in all examples is investigated via this wavelet.
- Since selecting the proper Laplacian filter has a considerable impression on the results of the Laplacian pyramid and contourlet transform, both filters 9/7 and PKVA, have been evaluated in this study to choose the qualified filter for the defect demonstration. As the 9/7 filter has better performance in comparison with the PKVA filter, it is considered in all examples to defect identification.
- As can be seen in Fig. 17, when there is a single defect in the plate, shearlet transform demonstrates excellent performance compared with the wavelet and Laplacian pyramid transform; however, the shearlet has a relatively similar function to the curvelet and contourlet transform. Therefore, it can be concluded that all these three transforms are useable tools to detect single damages in the plate structures.
- Based on the Fig. 17, wavelet, Laplacian pyramid, curvelet, and contourlet transform have poor ability to detect multiple damages with different shapes in plate structures. Nonetheless, the shearlet transform has shown the perfect ability to exhibit several damages on the plate.
- In conclusion, based on the numerical and experimental results, it could be concluded that the shearlet transform is a practical and efficient transform to identify all kinds of damages in the plate structures.

First to the Fourth Example				
Damage	 Point	 Horizontal linear	 Diagonal linear	 Curve
Laplacian pyramid				
Wavelet				
Curvelet				
Contourlet				
Shearlet				
Performance of the transforms in damage detection (First to the fourth example)	1) Wavelet: poor 2) Laplacian: poor 3) Curvelet: excellent 4) Contourlet: excellent 5) Shearlet: excellent	1) Wavelet: poor 2) Laplacian: poor 3) Curvelet: excellent 4) Contourlet: excellent 5) Shearlet: excellent	1) Wavelet: poor 2) Laplacian: poor 3) Curvelet: good 4) Contourlet: good 5) Shearlet: excellent	1) Wavelet: poor 2) Laplacian: poor 3) Curvelet: good 4) Contourlet: good 5) Shearlet: excellent

Fifth Example			
Damage			
Laplacian pyramid			
Wavelet			
Curvelet			
Contourlet			
Shearlet			
Sixth Example			
Damage			
Laplacian pyramid			
Wavelet			
Curvelet			

Contourlet			
Shearlet			

Seventh Example

Damage					
Laplacian pyramid					
Wavelet					
Curvelet					
Contourlet					
Shearlet					

Eighth Example						
Damage						
Laplacian pyramid					Not shown the damage	
Wavelet					Not shown the damage	
Curvelet					Not shown the damage	
Contourlet					Not shown the damage	
Shearlet					Not shown the damage	
Performance of the transforms in damage detection (Fifth to the eighth example)	1) Wavelet: poor 2) Laplacian: poor 3) Curvelet: poor 4) Contourlet: poor 5) Shearlet: excellent		1) Wavelet: poor 2) Laplacian: poor 3) Curvelet: poor 4) Contourlet: poor 5) Shearlet: excellent		1) Wavelet: poor 2) Laplacian: poor 3) Curvelet: poor 4) Contourlet: poor 5) Shearlet: excellent	

Fig. 17. The overall summary of the numerical examples.

There is the question of why the shearlet transform has superior efficiency in comparison with other transforms? To answer this question, let's consider two steps:

- First step: Comparison of shearlet with Laplacian pyramid and wavelet transform.

This section is summarized in three stages.

1. The capability to show more details causes better defect detection.
2. Shearlet has a better function to show details compared to Laplacian and wavelet transform.
3. Therefore, Shearlet has superior performance to exhibit defects.

These stages have been explained in detail as follows:

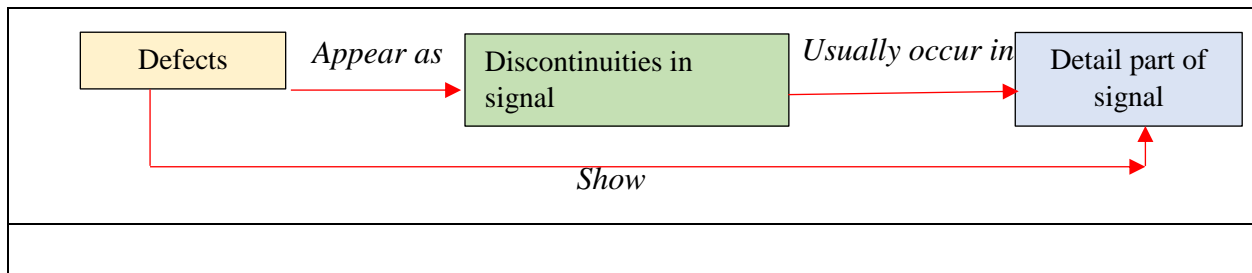


Fig. 18. The relationship between defects and detail part.

Consider Fig. 18; this Fig presents this fact that defects appear in discontinuities of signals. Discontinuities occur in the detail part. Therefore, to detect defects, we should find the detail part of a signal. Accordingly, each transform with the superior capability to illustrate details has better efficiency to display defects. Now the question is which of wavelet, Laplacian pyramid, and the shearlet transform can demonstrate the detail part more effectively. To find the answer see Fig. 19.

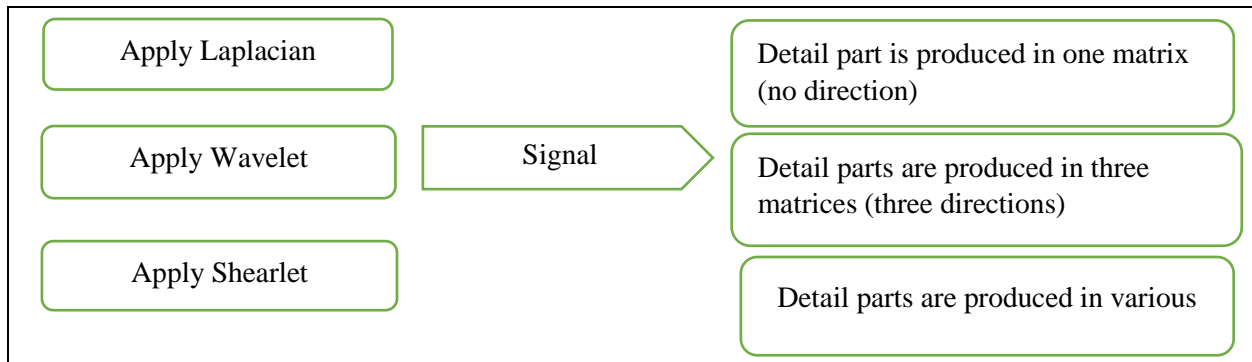


Fig. 19. The capability to show details.

As indicated in Fig. 19, the wavelet transform can demonstrate details in three directions (horizontal, vertical, and diagonal), which are three matrices. Also, the Laplacian pyramid can give the details in one matrix exclusively. Nonetheless, the shearlet transform can indicate detail coefficients in several diverse directions. Hence, shearlet demonstrates more details, providing superior performance to demonstrate damages.

- Second step: Comparison of shearlet with Curvelet and contourlet transform.

These three transforms can show details in various directions. It means they have the same ability to show details. Thus, there is a question of why shearlet has presented better performance to damage identification. The answer is the shape of basic elements, see Fig. 20.

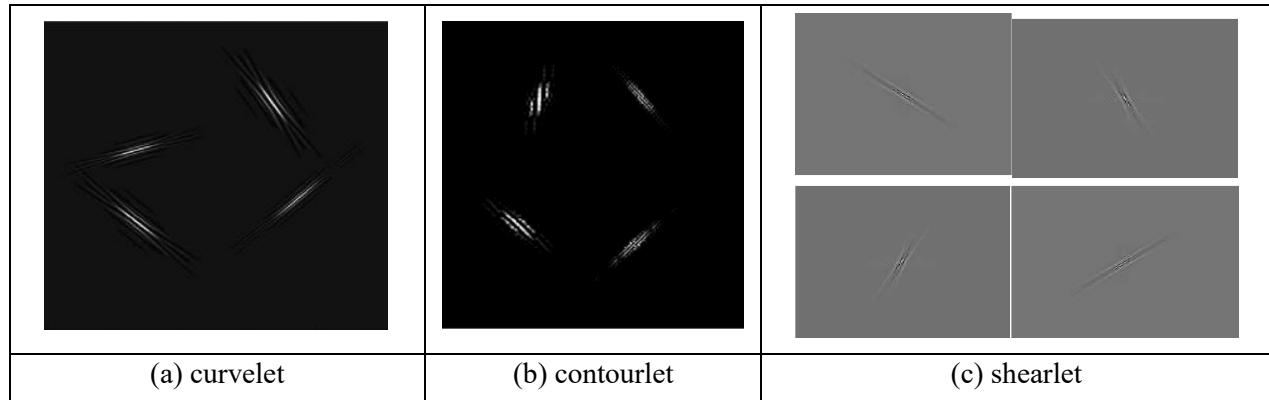


Fig. 20. The basic elements.

As shown in Fig. 20, each transform has elements with elongated shapes oriented in different directions; however, their basic forms are different. The shape of the basic elements of the shearlet transform is more proper to show defects; therefore, it offers a superior capability to detect damage.

6. Conclusions

This research proposed a new shearlet transform-based approach and compared it with four transforms, including wavelet, Laplacian pyramid, curvelet, and contourlet, to detect several types of damages, such as point, linear, and curve, in the plate structure. To assess, the performance of various wavelets; Haar, Symlet, and Discrete Meyer wavelets were applied, and the Discrete Meyer wavelet was considered the superior one. Also, 9/7 and PKVA filters were evaluated to find the best ability of contourlet transform to detect damages, and the 9/7 filter was considered the better one. Based on what was mentioned, the best performance of each transform was used to compare the results. According to numerical simulation results, wavelets and Laplacian Pyramid could not demonstrate curve defects perfectly. In addition, shearlet, curvelet, and contourlet transform have similar, excellent performance in the plate with single damage. However, only the shearlet demonstrates perfect performance to identify multiple defects in the plate structure. It is worth mentioning that signal-based methods have some limitations such as the inability to determine the severity of the damage. Hence, based on the results, the shearlet transform overcome the weakness of the wavelet transform. Also, it offered superior performance to the other multiresolution transforms (Laplacian Pyramid, curvelet, and contourlet) to detect damages with different shapes. In addition, the correctness of the shearlet transform was validated by the experimental example. Thus, the shearlet transform can be employed as an efficient and practicable tool for the detection of all types of damages.

Acknowledgments

The author would like to thank Professor Rucka and Wilde for providing the experimental data, and Professor Forgoston for his constructive feedback on the paper.

Funding

This research received no external funding.

Conflicts of interest

The authors declare no conflict of interest.

References

- [1] Ovanesoava A V, Suarez LE. Applications of wavelet transforms to damage detection in frame structures. *Eng Struct* 2004;26:39–49. <https://doi.org/10.1016/j.engstruct.2003.08.009>.
- [2] Kim H, Melhem H. Damage detection of structures by wavelet analysis. *Eng Struct* 2004;26:347–62. <https://doi.org/10.1016/j.engstruct.2003.10.008>.
- [3] Yun GJ, Lee S-G, Carletta J, Nagayama T. Decentralized damage identification using wavelet signal analysis embedded on wireless smart sensors. *Eng Struct* 2011;33:2162–72. <https://doi.org/10.1016/j.engstruct.2011.03.007>.
- [4] Bagheri A, Ghodrati Amiri G, Khorasani M, Bakhshi H. Structural damage identification of plates based on modal data using 2D discrete wavelet transform. *Struct Eng Mech* 2011;40:13–28. <https://doi.org/10.12989/sem.2011.40.1.013>.
- [5] Cao M, Xu W, Ostachowicz W, Su Z. Damage identification for beams in noisy conditions based on Teager energy operator-wavelet transform modal curvature. *J Sound Vib* 2014;333:1543–53. <https://doi.org/10.1016/j.jsv.2013.11.003>.
- [6] Yongchao Y, Nagarajaiah S. Blind identification of damage in time-varying system using independent component analysis with wavelet transform", *J. Mech Syst Signal Process* 2012;27:3–20. <https://doi.org/10.1016/j.ymsp.2012.08.029>.
- [7] Ulriksen MD, Tcherniak D, Kirkegaard PH, Damkilde L. Operational modal analysis and wavelet transformation for damage identification in wind turbine blades. *Struct Heal Monit* 2016;15:381–8. <https://doi.org/10.1177/1475921715586623>.
- [8] Shahsavari V, Chouinard L, Bastien J. Wavelet-based analysis of mode shapes for statistical detection and localization of damage in beams using likelihood ratio test. *Eng Struct* 2017;132:494–507. <https://doi.org/10.1016/j.engstruct.2016.11.056>.
- [9] Wang S, Li J, Luo H, Zhu H. Damage identification in underground tunnel structures with wavelet based residual force vector. *Eng Struct* 2019;178:506–20. <https://doi.org/10.1016/j.engstruct.2018.10.021>.

- [10] Zhu L-F, Ke L-L, Zhu X-Q, Xiang Y, Wang Y-S. Crack identification of functionally graded beams using continuous wavelet transform. *Compos Struct* 2019;210:473–85. <https://doi.org/10.1016/j.compstruct.2018.11.042>.
- [11] Jahangir H, Hasani H, Esfahani MR. Damage Localization of RC Beams via Wavelet Analysis of Noise Contaminated Modal Curvatures. *J Soft Comput Civ Eng* 2021;5:101–33. <https://doi.org/10.22115/scce.2021.292279.1340>.
- [12] Pouyan F, Hosein N. Damage Severity Quantification Using Wavelet Packet Transform and Peak Picking Method. *Pract Period Struct Des Constr* 2022;27:4021063. [https://doi.org/10.1061/\(ASCE\)SC.1943-5576.0000639](https://doi.org/10.1061/(ASCE)SC.1943-5576.0000639).
- [13] Naderpour H, Sharei M, Fakharian P, Heravi MA. Shear Strength Prediction of Reinforced Concrete Shear Wall Using ANN, GMDH-NN and GEP. *J Soft Comput Civ Eng* 2022;6:66–87. <https://doi.org/10.22115/scce.2022.283486.1308>.
- [14] Ghanizadeh AR, Delaram A, Fakharian P, Armaghani DJ. Developing Predictive Models of Collapse Settlement and Coefficient of Stress Release of Sandy-Gravel Soil via Evolutionary Polynomial Regression. *Appl Sci* 2022;12:9986. <https://doi.org/10.3390/app12199986>.
- [15] Naderpour H, Rezazadeh Eidgahee D, Fakharian P, Rafiean AH, Kalantari SM. A new proposed approach for moment capacity estimation of ferrocement members using Group Method of Data Handling. *Eng Sci Technol an Int J* 2020;23:382–91. <https://doi.org/10.1016/j.jestch.2019.05.013>.
- [16] Bagheri A, Kourehli S. Damage detection of structures under earthquake excitation using discrete wavelet analysis. *Asian J Civ Eng* 2013.
- [17] Kourehli SS. Health Monitoring of Connections in Steel Frames Using Wavelet Transform. *Amirkabir J Civ Eng* 2020;52:655–72. <https://doi.org/10.22060/ceej.2018.14815.5750>.
- [18] Ghannadi P, Kourehli SS. Efficiency of the slime mold algorithm for damage detection of large-scale structures. *Struct Des Tall Spec Build* 2022;31:e1967. <https://doi.org/10.1002/tal.1967>.
- [19] Ghannadi P, Kourehli SS. Structural damage detection based on MAC flexibility and frequency using moth-flame algorithm. *Struct Eng Mech* 2019;70:649–59. <https://doi.org/10.12989/sem.2019.70.6.649>.
- [20] Ghannadi P, Kourehli SS. Model updating and damage detection in multi-story shear frames using salp swarm algorithm. *Earthquakes Struct* 2019;17:63–73. <https://doi.org/10.12989/eas.2019.17.1.063>.
- [21] Ghannadi P, Kourehli SS, Noori M, Altabey WA. Efficiency of grey wolf optimization algorithm for damage detection of skeletal structures via expanded mode shapes. *Adv Struct Eng* 2020;23:2850–65. <https://doi.org/10.1177/1369433220921000>.
- [22] Ghannadi P, Kourehli SS. Multiverse optimizer for structural damage detection: Numerical study and experimental validation. *Struct Des Tall Spec Build* 2020;29:e1777. <https://doi.org/10.1002/tal.1777>.
- [23] Ghannadi P, Kourehli SS, Mirjalili S. The Application of PSO in Structural Damage Detection: An Analysis of the Previously Released Publications (2005–2020). *Frat Ed Integrità Strutt* 2022;16:460–89. <https://doi.org/10.3221/IGF-ESIS.62.32>.

- [24] BURT PJ, ADELSON EH. The Laplacian Pyramid as a Compact Image Code. In: Fischler MA, Firschein OBT-R in CV, editors., San Francisco (CA): Morgan Kaufmann; 1987, p. 671–9. <https://doi.org/10.1016/B978-0-08-051581-6.50065-9>.
- [25] Do MN, Vetterli M. Contourlets. In: Welland GVB-T-S in CM, editor. *Beyond Wavelets*, vol. 10, Elsevier; 2003, p. 83–105. [https://doi.org/10.1016/S1570-579X\(03\)80032-0](https://doi.org/10.1016/S1570-579X(03)80032-0).
- [26] Candès E, Demanet L, Donoho D, Ying L. Fast Discrete Curvelet Transforms. *Multiscale Model Simul* 2006;5:861–99. <https://doi.org/10.1137/05064182X>.
- [27] Bagheri A, Ghodrati Amiri G, Seyed Razzaghi SA. Vibration-based damage identification of plate structures via curvelet transform. *J Sound Vib* 2009;327:593–603. <https://doi.org/10.1016/j.jsv.2009.06.019>.
- [28] Nicknam A, Hosseini MH, Bagheri A. Damage detection and denoising in two-dimensional structures using curvelet transform by wrapping method. *Arch Appl Mech* 2011;81:1915–24. <https://doi.org/10.1007/s00419-011-0527-y>.
- [29] Do MN, Vetterli M. The contourlet transform: an efficient directional multiresolution image representation. *Off Journal-European Union Inf Not C* 2006;49:2091. <https://doi.org/10.1109/TIP.2005.859376>.
- [30] Po DD-Y, Do MN. Directional multiscale modeling of images using the contourlet transform. *IEEE Trans Image Process* 2006;15:1610–20. <https://doi.org/10.1109/TIP.2006.873450>.
- [31] Vafaie S, Salajegheh E. Comparisons of wavelets and contourlets for vibration-based damage identification in the plate structures. *Adv Struct Eng* 2019;22:1672–84. <https://doi.org/10.1177/1369433218824903>.
- [32] Jahangir H, Khatibinia M, Kavousi M. Application of Contourlet Transform in Damage Localization and Severity Assessment of Prestressed Concrete Slabs. *J Soft Comput Civ Eng* 2021;5:39–67. <https://doi.org/10.22115/scce.2021.282138.1301>.
- [33] Lim W-Q. The Discrete Shearlet Transform: A New Directional Transform and Compactly Supported Shearlet Frames. *IEEE Trans Image Process* 2010;19:1166–80. <https://doi.org/10.1109/TIP.2010.2041410>.
- [34] Xu K, Liu S, Ai Y. Application of Shearlet transform to classification of surface defects for metals. *Image Vis Comput* 2015;35:23–30. <https://doi.org/https://doi.org/10.1016/j.imavis.2015.01.001>.
- [35] Chopra AK. *Dynamics of structures*. Pearson Education India; 2007.
- [36] Kailath T. An innovations approach to least-squares estimation--Part I: Linear filtering in additive white noise. *IEEE Trans Automat Contr* 1968;13:646–55. <https://doi.org/10.1109/TAC.1968.1099025>.
- [37] Daubechies I. *Ten Lectures on Wavelets*. vol. 1. Society for Industrial and Applied Mathematics; 1992. <https://doi.org/10.1137/1.9781611970104>.
- [38] Rhif M, Abbes A Ben, Farah IR, Martínez B, Sang Y. Wavelet transform application for/in non-stationary time-series analysis: A review. *Appl Sci* 2019;9:1–22. <https://doi.org/10.3390/app9071345>.
- [39] Meyer Y. *Wavelets and Operators: Volume 1*. Cambridge university press; 1992.
- [40] Candes EJ, Donoho DL. *Curvelets: A surprisingly effective nonadaptive representation for objects with edges*. Stanford Univ Ca Dept of Statistics; 2000.

- [41] Easley G, Labate D, Lim W-Q. Sparse directional image representations using the discrete shearlet transform. *Appl Comput Harmon Anal* 2008;25:25–46. <https://doi.org/https://doi.org/10.1016/j.acha.2007.09.003>.
- [42] Vyas A, Yu S, Paik J. *Multiscale Transforms with Application to Image Processing*. Singapore: Springer Singapore; 2018. <https://doi.org/10.1007/978-981-10-7272-7>.
- [43] Rucka M, Wilde K. Application of continuous wavelet transform in vibration based damage detection method for beams and plates. *J Sound Vib* 2006;297:536–50. <https://doi.org/https://doi.org/10.1016/j.jsv.2006.04.015>.
- [44] Ghannadi P, Kourehli SS. Data-driven method of damage detection using sparse sensors installation by SEREPa. *J Civ Struct Heal Monit* 2019;9:459–75. <https://doi.org/10.1007/s13349-019-00345-8>.
- [45] Ghannadi P, Kourehli SS. An effective method for damage assessment based on limited measured locations in skeletal structures. *Adv Struct Eng* 2021;24:183–95. <https://doi.org/10.1177/1369433220947193>.
- [46] Chen Y, Logan P, Avitabile P, Dodson J. Non-Model Based Expansion from Limited Points to an Augmented Set of Points Using Chebyshev Polynomials. *Exp Tech* 2019;43:521–43. <https://doi.org/10.1007/s40799-018-00300-0>.